



## **Evaluation of power control with different electrical and control concept of wind farm Part 2 – Large systems**

**Hansen, Anca Daniela**

*Publication date:*  
2010

*Document Version*  
Publisher's PDF, also known as Version of record

[Link back to DTU Orbit](#)

*Citation (APA):*  
Hansen, A. D. (2010). *Evaluation of power control with different electrical and control concept of wind farm: Part 2 – Large systems*. Project UpWind.

---

### **General rights**

Copyright and moral rights for the publications made accessible in the public portal are retained by the authors and/or other copyright owners and it is a condition of accessing publications that users recognise and abide by the legal requirements associated with these rights.

- Users may download and print one copy of any publication from the public portal for the purpose of private study or research.
- You may not further distribute the material or use it for any profit-making activity or commercial gain
- You may freely distribute the URL identifying the publication in the public portal

If you believe that this document breaches copyright please contact us providing details, and we will remove access to the work immediately and investigate your claim.



Project funded by the European Commission under the 6th (EC) RTD Framework Programme (2002- 2006) within the framework of the specific research and technological development programme "Integrating and strengthening the European Research Area"



## Project UpWind

Contract No.:  
019945 (SES6)

"Integrated Wind Turbine Design"



---

### Work Package 9: Electrical grid

#### Deliverable D 9.4.4

#### Evaluation of power control

with different electrical and control concept of wind farm

#### Part 2 – Large systems

---

AUTHORS:	Anca D. Hansen
AFFILIATION:	Risø National Laboratory for Sustainable Energy
ADDRESS:	Frederiksborgvej 399, P.O. Box 49, Building 125, 4000 Roskilde, Denmark
TEL.:	+45 4677 5073
EMAIL:	anca@risoe.dtu.dk
FURTHER AUTHORS:	
REVIEWER:	Poul Sørensen
APPROVER:	Poul Sørensen

*Document Information*

DOCUMENT TYPE	Report
DOCUMENT NAME:	Evaluation of power control with different electrical and control concept of wind farm
DOCUMENT NUMBER:	
REVISION:	<b>FINAL</b>
REV.DATE:	April 2010
CLASSIFICATION:	R0 (General Public)
STATUS:	FINAL

**Abstract:**

This report investigates the impact of wind power in large power systems.

The motivation for this investigation is the ever-increasing wind energy penetration into the power systems throughout the world. A generic large power system model delivered by the Danish Transmission System Operator Energinet.dk is used in the presented study cases.

# Contents

---

<b>1.</b>	<b>Introduction.....</b>	<b>3</b>
<b>2.</b>	<b>Grid code requirements.....</b>	<b>5</b>
2.1.	Fault ride-through capability .....	5
2.2.	Power control capability.....	7
<b>3.</b>	<b>Wind farm models.....</b>	<b>10</b>
3.1	Active stall wind turbine.....	15
3.2	Doubly-fed induction generator wind turbine.....	23
3.3	Multi-pole PMSG wind turbine grid support.....	34
<b>4.</b>	<b>Generic large power system model.....</b>	<b>44</b>
<b>5.</b>	<b>Fault ride-through capability.....</b>	<b>49</b>
5.1.	ASIG wind turbines' response to grid faults .....	49
5.2.	DFIG wind turbines' response to grid faults .....	51
3.4	Multi-pole PMSG wind turbines' response to grid faults .....	59
<b>6.</b>	<b>Power grid support .....</b>	<b>62</b>
6.1	ASIG wind turbine's power grid support.....	62
6.2	DFIG wind turbines' power grid support .....	68
6.3	Multi-pole PMSG wind turbines' power grid support.....	72
<b>7.</b>	<b>Voltage grid support.....</b>	<b>73</b>
7.1.	ASIG wind turbines' voltage grid support .....	74
7.2.	DFIG wind turbines' voltage grid support .....	76
7.3.	Multi-pole PMSG wind turbines' voltage grid support.....	81
<b>8.</b>	<b>Conclusions.....</b>	<b>85</b>

STATUS, CONFIDENTIALITY AND ACCESSIBILITY							
Status			Confidentiality			Accessibility	
<b>S0</b>	Approved/Released		<b>R0</b>	General public	(X)	Private web site	
<b>S1</b>	Reviewed		<b>R1</b>	Restricted to project members		Public web site	(X)
<b>S2</b>	Pending for review		<b>R2</b>	Restricted to European. Commission		Paper copy	
<b>S3</b>	Draft for comments	X	<b>R3</b>	Restricted to WP members + PL			
<b>S4</b>	Under preparation		<b>R4</b>	Restricted to Task members +WPL+PL			

**PL:** Project leader**WPL:** Work package leader**TL:** Task leader

# 1. Introduction

The motivation for this investigation is the ever-increasing wind energy penetration into the power systems throughout the world. Wind power, as most of the renewable energy sources, possesses a different role in the power system compared to conventional power generation units. As long as only single and small wind power units are installed in the power system, wind power does not influence power system operation and can easily be integrated. However, when wind power penetration reaches a significant high level and conventional power production units are substituted, the impact of wind power on the power system becomes noticeable and must be handled.

The connection of large wind turbines and wind farms to the grid has a large impact on grid stability. The electrical power system becomes more vulnerable to and dependent on the wind energy production, and therefore there is an increased concern about the large wind turbines impact's on grid stability. This situation, which implies new challenges for power system operators to ensure reliable and stable grid operation, is directly reflected in the requirements for grid connections of the wind turbines. These codes are getting more and more demanding, requiring wind farms to behave more and more as conventional power plants in the power system and to have thus more responsibility in network operation. The status of wind turbines is thus changing from being simple energy sources to having power plant status. This means that sooner or later, they will have to share some of the duties carried out today by the conventional power plants, namely behave as active controllable components in the power system, i.e. regulating active and reactive power and performing frequency and voltage control on the grid.

The increased penetration of wind power has challenged not only the power system operators but also different wind turbine manufactures. It has initiated as result an important research activity directed towards connecting and optimised integration of large wind farms within the electrical power grid.

The wind turbine technology and complex wind turbines/wind farms control strategies have been rapidly developed over the past few years. Today, the wind turbines on the market mix and match a variety of innovative concepts with proven technologies for both

generators and power electronics [1-2]. The survival of these wind turbine technologies is strongly conditioned by their ability to support the grid, to handle faults on the grid and to comply with the stringent requirements of the utility companies. These requirements are determined for wind farms connected to the transmission grid, but they apply both to onshore and offshore farms.

The main trend of modern wind turbines/wind farms is clearly the variable speed operation and a grid connection through power electronic interfaces. The presence of power electronics inside wind turbines/wind farms offers enlarged control capabilities to the wind farms to fulfill the grid requirements. During the last years, the market interest for the fixed speed active stall wind turbine concept has therefore decreased slightly in favour of variable speed wind turbine concepts. One reason for that is that they do not contain advanced power-electronic components and their control is typically not designed to support the grid. However, they are still attractive due to their robustness, simplicity and low cost. The market interest for wind farms with active stall turbines may therefore increase if their grid support is improved.

Consequently, there is much worldwide research investigating the suitability of different wind turbine concepts to comply with the grid utilities requirements [3-4]. The recent development of large wind farms and their integration into the power system has furthermore initiated an important research activity in the development of modern advanced wind farm controllers adapted to each specific wind turbine technology.

This study deals with the impact on large power systems of different wind turbine concepts like active stall induction generator (ASIG) wind turbines, doubly-fed induction generator (DFIG) wind turbines and multi-pole permanent magnet synchronous generator (PMSG) wind turbines, when they are equipped with advanced controllers designed to comply with the grid code requirements.

The present investigation focuses on the most relevant features regarding integration of wind power into large power systems, i.e. fault ride through, power control and voltage support control capabilities of different wind farm concepts. As large power systems have typically large generator inertia included, frequency stability problem is not a special issue as in case of small autonomous power systems and it is therefore not addressed in the report.



## 2. Grid code requirements

The connection of large wind turbines to the grid has a large impact on grid stability. The increased penetration of wind energy into the power system over the last decade has therefore led to serious concern about its influence on the dynamic behavior of the power system. It has resulted in the power system operators revising and increasing the grid connection requirements in several countries. An overview of the national grid requirements in countries as Denmark, Ireland, Germany, Great Britain, Spain, Italy, USA and Canada is also provided in [5].

The main attention in the grid requirements is drawn to the fault ride-through and power control capabilities of large wind farms.

### 2.1. Fault ride-through capability

The fault ride-through requirement has been imposed in order to avoid significant loss of wind turbine production in the event of grid faults. Up to 7-8 years ago, wind turbines were only required to be disconnected from the grid when a grid fault was detected, in order thus to avoid large inrush currents when the voltage recovered. However, with the increased capacity of wind power in the power system over the years, such a disconnection of wind turbines could generate control problems of frequency and voltage in the system, and as worst case a system collapse.

The fault ride-through capability addresses primarily the design of the wind turbine controller in such a way that the wind turbine is able to remain grid-connected during grid faults. The fault ride-through demand is also a challenge on how to recover the voltage after a grid fault. This is especially the case of wind turbines with squirrel cage induction generator which, by being kept connected to the grid during grid faults may require large currents to energize their induction generators, when the voltage returns after a while. This can lead to possible violation of grid codes and security standards.

The fault ride-through capability depends on the particular wind turbine technology. The early generation of wind turbines would disconnect from the grid even during quite small disturbances as they did not have any fault ride-through capability, in accordance with the grid codes that were valid at the time of their installation. Modern wind turbines,

e.g. those with doubly fed induction generator (DFIG) are able to stay connected during and after the fault, if they are equipped with a frequency converter protection system. Furthermore, they are able to support the power system and even improve the behaviour of local wind turbines with conventional technology, if they are equipped with appropriate control for grid support [6].

A summary of the fault ride-through requirement in different national grid codes is given in Table 1. Notice that some national grid codes e.g. Denmark and Ireland have specific fault ride-through requirements for distribution networks as well as for transmission ones, while other national grid codes have focus only on the transmission level. The voltage profiles in these national requirements are given specifying the depth of the voltage drop and the clearance time as well. In some of the grid requirements, as in Denmark, Ireland and Germany, the definition of the voltage profile is clearly specified regarding the type of the fault, i.e. symmetric or asymmetric.

**Table 1: Summary of national fault ride-through requirements - source [5].**

Country	Voltage Level	Fault ride-through capability				
		Fault duration	Voltage drop level	Recovery time	Voltage profile	Reactive current injection
Denmark	DS	100 msec	25% $U_r$	1 sec	2, 3-ph	no
	TS	100 msec	25% $U_r$	1 sec	1, 2, 3-ph	no
Ireland	DS/TS	625 msec	15% $U_r$	3 sec	1, 2, 3- ph	no
Germany	TS	150 msec	0% $U_r$	1.5 sec	generic	Up to 100%
Great Britain	TS	140msec	15% $U_r$	1.2sec	generic	no
Spain	TS	500 msec	20% $U_r$	1 sec	generic	Up to 100%
Italy	> 35 kV	500 msec	20% $U_r$	0.3 sec	generic	no
USA	TS	625 msec	15% $U_r$	2.3 sec	generic	no
Ontario	TS	625 msec	15% $U_r$	-	-	no
Quebec	TS	150 msec	0% $U_r$	0.18 sec	Positive-sequence	no

Notice that there is a significant span in the fault ride-through requirements in different countries. For example, the fault duration varies from 100 msec (in Denmark) to 625 msec (in Ireland, USA and Canada), while the voltage drop level down varies between 25% to even 0% of the nominal value. The Ireland's code is very demanding regarding

the fault duration, while Denmark has the lowest fault duration with only 100msec. However, Denmark's code requires the wind turbine to remain connected to the grid during successive faults. The German grid code requires the wind turbines to remain connected to the grid during voltage sags down to 0% from the rated voltage in the PCC for a duration of 150msec. Moreover, a reactive current injection up to 100% during fault is required, this requirement being also present in the Spanish grid code.

## **2.2. Power control capability**

The power control ability means mainly that the wind turbines have to share, for shorter or longer periods, some of the duties carried out traditionally by conventional power plants, such as regulating active and reactive power and performing frequency and voltage control on the grid.

The power control capabilities requirements correspond basically to the wind farm controllers implemented for the two large Danish wind farms, namely 160MW Horns Rev wind farm [7] and 165MW Nysted wind farm. These large wind farms are equipped with capable power control features with remote access. Even though they are consisting of different wind turbine concepts, having thus different dynamic response to the control request, their power control behaviour is quite similar.

The power control requirements regard different power system control and stability aspects:

- ***active power/frequency control ability*** with focus on:
  - *primary control* – is a fast, automatic global adjustment of power to frequency.
  - *secondary control* – is a slower, automatic or manual regional regulation of the power to the power reference imposed by the system operator at any time.
- ***reactive power/voltage control ability*** with focus on voltage regulation and reactive power capability.
- ***dynamic stability*** with focus on the ability of wind farms to withstand some specific grid faults without being disconnected.

Modern wind farms have to provide advanced grid support [7-8], such as the following different control functions, illustrated in Figure 1:

- *Balance control* – whereby the wind farm production can be adjusted downwards or upwards, in steps at constant levels.
- *Delta control* – whereby the wind farm is ordered to operate with a certain constant reserve capacity in relation to its momentary possible power production capacity.
- *Power gradient limiter* – which sets how fast the wind farm power production can be adjusted upwards and downwards.
- *Automatic frequency control* – whereby the wind farm must be able to produce more or less active power in order to compensate for a possible deviant behaviour in the frequency measured in the wind farm point of common coupling (PCC).
- *Reactive power control* – whereby the wind farm is required to produce or absorb a constant specific amount of reactive power.
- *Automatic voltage control* – whereby the wind farm automatically produces or consumes an amount of reactive power in order to control the voltage in the point of common coupling (PCC) of the wind farm.

The power system operators are not only requiring power plant characteristics for the wind turbines, but also development of suitable dynamic models to assess the wind generation impact on system stability. Such models play an important role in the design of national grid codes. Various wind turbine manufactures have also been challenged to initiate research activities directed towards connection and optimised integration of large wind farms within the electrical power grid. Risø-DTU National Laboratory has developed a dynamic simulation model for wind farms [6], [9-10], including both wind farm controllers, individual wind turbine controllers and the dynamics of the wind turbines themselves.

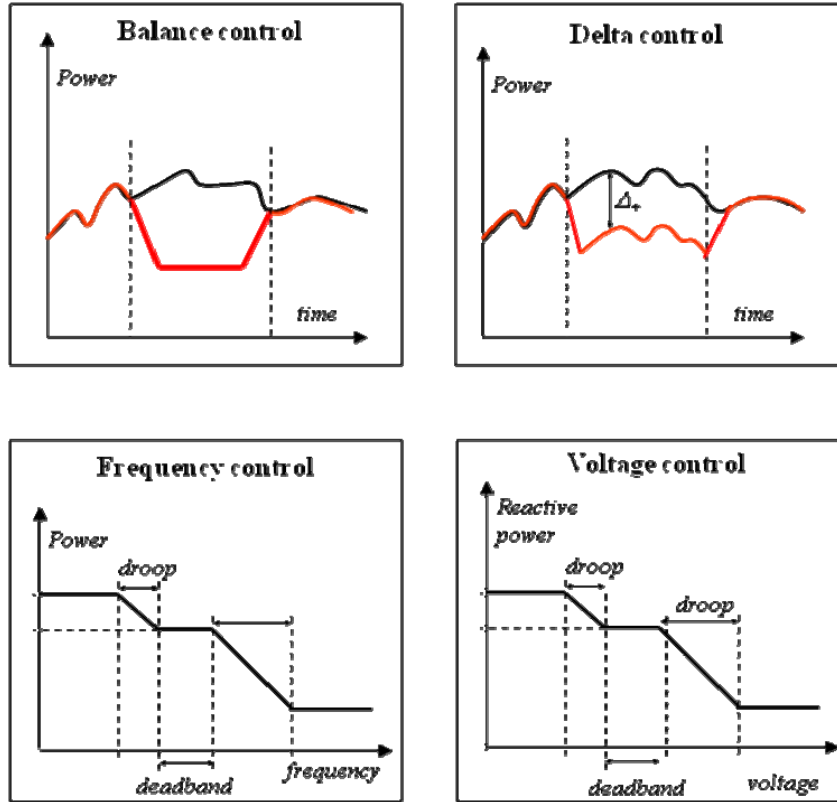


Figure 1: Different control functions in modern wind farms.

Figure 2 illustrates the general structure of such wind farm model, which is similar to what is actually implemented in the Danish Horn Rev and Nysted farms. All the demands illustrated in Figure 1, can be imposed by the power system operator to the wind farm controller. The wind farm controller controls the power production from the whole wind farm by issuing instructions (power references) to each individual wind turbine, each of which having its own controller. These instructions are prepared based on the power system demands, measurements in PCC and on the received information from the wind turbines about the maximum amount of available power.

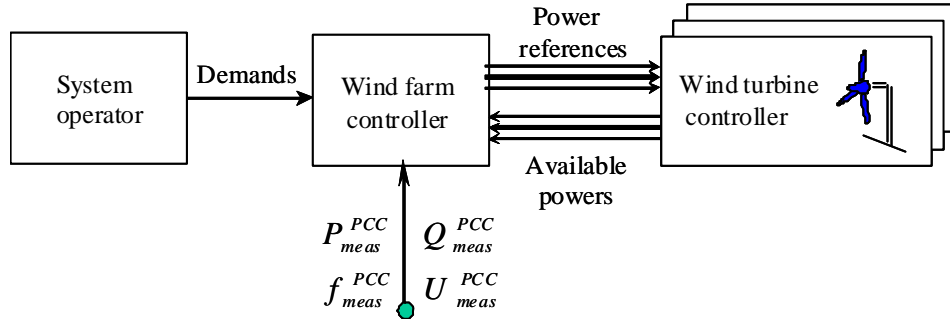


Figure 2: The general structure of a wind farm control system.

### 3. Wind farm models

This chapter summarizes the work done on modeling and development of the dynamic control of the wind farms. Models and control strategies for three different types of wind farms have been developed, with the aim to optimize the operation of the wind farms considering their participation in the grid support (fault ride-through, active and reactive power control, frequency control and voltage control). Models and control for three different types of wind turbines have been developed:

- Fixed speed active stall wind turbine concept
- Variable speed doubly-fed induction generator wind turbine concept
- Variable speed multi-pole permanent magnet synchronous generator wind turbine concept

These wind turbine concept models can be used and even extended for the study of different aspects, e.g. the assessment of power quality, control strategies, connection of the wind turbine at different types of grid and storage systems. Different control strategies have been developed and implemented for these wind turbine concepts, their performance in normal or fault operation being assessed and discussed by means of simulations.

A simplified block scheme of the wind turbine models is shown in Figure 3. The basic block scheme of the wind turbine consists of a wind model, an aerodynamic model, a transmission system, generator model and a control block model.

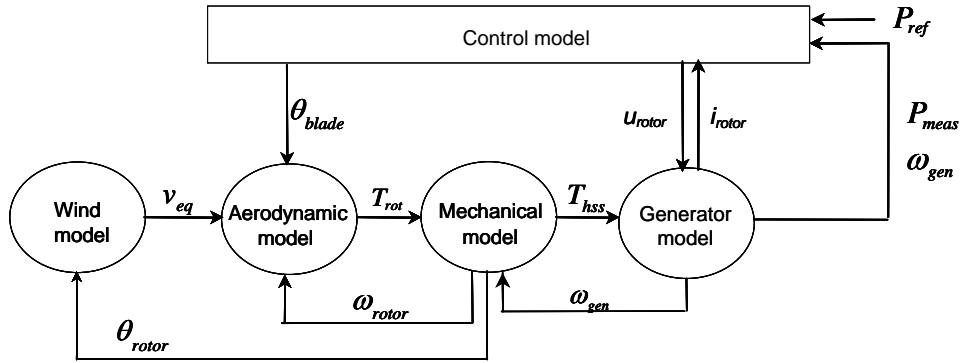


Figure 3: Scheme of wind turbine models.

## I. Wind model

The wind model used is described in detail in [11]. The main advantages of this wind model are the fast computation, reduced memory requirements and the ease of use, either for variable or constant speed models. This wind speed model is very suitable for simultaneous simulation of a large number of wind turbines, making it possible to estimate efficiently the impact of a large wind farm on the power quality.

The structure of the wind model is shown in Figure 4. It provides an equivalent wind speed  $v_{eq}$  to the aerodynamic model. The wind model includes two sub-models: a hub wind model and a rotor wind model.

The hub wind model models the fixed-point wind speed at hub height for each wind turbine. In this hub wind model, the park scale coherence is taken into account in the case when a whole wind farm is modeled. The second is the rotor wind model, which includes the averaging effect of the wind speeds over the whole rotor, the rotational sampling effect, and a tower shadow model. The wind shear is not included in the rotor wind model, as it only has a small influence on the power fluctuations.

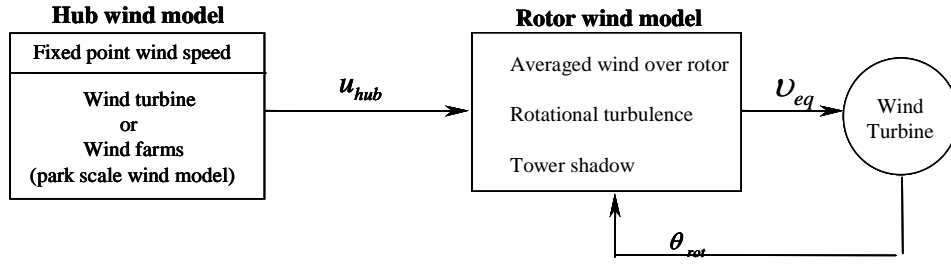


Figure 4: Structure of the wind model.

Notice that the rotor position  $\theta_{rot}$  is used in the wind model, and therefore this wind model can be used both variable speed and constant speed.

## II. Mechanical model

In the mechanical model, the emphasis is put only on those parts of the dynamic structure of the wind turbine that contribute to the interaction with the grid. Therefore only the drive train is considered in the first place, because this part of the wind turbine has the most significant influence on the power fluctuations. The other parts of the wind turbine structure, e.g. tower and the flap bending modes are neglected.

The mechanical model is shown in Figure 5. It is essentially a two mass model connected by a flexible low-speed shaft characterized by a stiffness  $k$  and a damping  $c$ . The high-speed shaft is assumed stiff. Moreover, an ideal gear with the exchange ratio  $1:n$  gear is included.

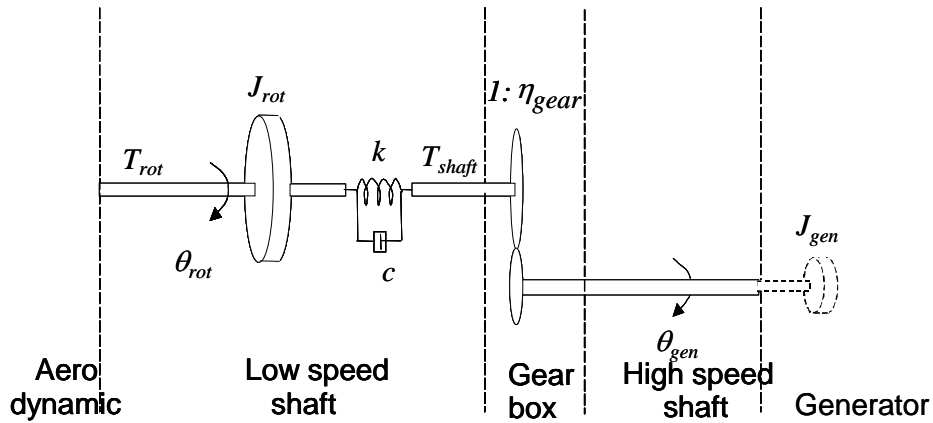


Figure 5: Mechanical model of wind turbine drive train.



The two masses correspond to the large turbine rotor inertia  $J_{rot}$ , representing the blades and hub, and to the small inertia  $J_{gen}$  representing the induction generator. The generator inertia is actually included in the generator models in DIgSILENT.

The drive train converts the aerodynamic torque  $T_{rot}$  of the rotor into the torque on the low speed shaft  $T_{shaft}$ . The dynamical description of the mechanical model consists of three differential equations, namely:

$$\begin{aligned}\dot{\theta}_{rot} &= \omega_{rot} & [rad / s] \\ \dot{\theta}_k &= \omega_{rot} - \frac{\omega_{gen}}{n_{gear}} & [rad / s] \\ \dot{\omega}_{rot} &= (T_{rot} - T_{shaft}) / J_{rot} & [rad / s^2]\end{aligned}\tag{1}$$

Where  $\theta_k = \theta_{rot} - \theta_{gen} / n_{gear}$  is the angular difference between the two ends of the flexible shaft. The mechanical torque on the low speed shaft and the mechanical power of the generator are:

$$\begin{aligned}T_{shaft} &= c \left( \omega_{rot} - \frac{\omega_{gen}}{n_{gear}} \right) + k \theta_k & [Nm] \\ P_t &= \omega_{gen} \frac{T_{shaft}}{n_{gear}} & [W]\end{aligned}\tag{2}$$

The damping coefficient  $c$  is given by:

$$c = 2 \xi \sqrt{k J_{rot}}\tag{3}$$

where  $\xi$  is the damping ratio and can be expressed using the logarithmic decrement  $\delta_s$ :

$$\xi = \frac{\delta_s}{\sqrt{\delta_s^2 + 4 \pi^2}}\tag{4}$$

The logarithmic decrement is the logarithm of the ratio between the amplitude at the beginning of the period and the amplitude at the end of the next period of the oscillation:

$$\delta_s = \ln \left( \frac{a(t)}{a(t+t_p)} \right) \quad (5)$$

where  $a$  denotes the amplitude of the signal.

### III. Aerodynamic model

The aerodynamic model is based on tables with the aerodynamic power efficiency  $C_p(\theta, \lambda)$  or torque coefficient  $C_q(\theta, \lambda)$ , which depend on the pitch angle  $\theta$  and on the tip speed ratio  $\lambda$ . This is a quasistatic aerodynamic model which determines the output aerodynamic torque directly from the input wind speed according to:

$$T_{rot} = \frac{P_{rot}}{\omega_{rot}} = \frac{1}{2} \rho \pi R^2 u^3 C_p(\theta, \lambda) \quad \text{a)}$$

or

$$T_{rot} = \frac{1}{2} \rho \pi R^3 u^2 C_q(\theta, \lambda) \quad \text{b)}$$

The aerodynamic model can also include a model for dynamic stall as described in [12]. The implemented model for dynamic stall is based on Øye's dynamic stall model [13].

### IV. Aggregation modeling

Aggregated modeling of large wind farms is commonly used to facilitate the investigation of the impact of a large wind farm on the dynamics of the power system to which it is connected. This type of modeling is often used in system studies where the concern is not on the individual wind turbines but on the impact of the entire farm on the power system. The advantage of an aggregated model is that it eliminates the need to develop a detailed model of the wind farm with tens or hundreds of wind turbines and their interconnections and that it reduces both the complexity of the system and the computation time substantially.

The idea of the aggregation is to represent an entire large wind farm in voltage stability investigations by one equivalent lumped wind turbine with re-scaled power capacity. According to [14], the mutual interaction between converter control systems of the wind turbines equipped with the DFIG can be neglected.

PowerFactory DIgSILENT offers a built-in directly aggregation technique for the electrical system (i.e. generator, power converter, transformer, capacitor, inductance) of the wind turbine [15]: for example, the generator and the transformers, can be modeled directly by a certain number of parallel machines or transformers, respectively, while the other electrical components (power converter, capacitance, inductance) and control can be up scaled accordingly to the increased power flow. The mechanical part of the wind farm aggregated model, namely the shaft model, the aerodynamics and the pitch system, is modeled as for one individual wind turbine. The mechanical power used as input to the aggregated generator is then the mechanical output from one turbine multiplied with the number of turbines in the wind farm.

### **3.1 Active stall wind turbine**

Two versions of models for the active stall controlled wind turbine have been developed and used at Risø-DTU National Laboratory. The two models reflect the wind turbine development and according to requirements in e.g. the Danish grid codes.

The first version described in [16] was developed to simulate the first generation of active stall / combi stall turbines. Originally, the concept was developed because the blades became too big for tip breakers, and therefore the whole blade had to become pitchable. This pitch was further used to remove one of the problems with passive stall, namely that the maximum power and maximum shaft torque cannot be controlled actively, since the maximum power of a passive stall controlled wind turbine is influenced e.g. by weather conditions (air density) and grid frequency. This first generation of active stall controlled wind turbines would reduce the pitch activity to a minimum, and thus had a relatively slow power control. Also reactive power control was slow, because the capacitor bank used mechanical contactors.

The second model described in [10] was optimized for grid support, and it is in that respect expected to be quite similar to the Nysted wind turbine. On the active power

control side, it responds within a few seconds to changes in the power set point, and on the reactive power side, it assumes dynamic phase compensation using a thyristor switched capacitor bank.

Figure 6 illustrates a typical example layout of the active stall wind turbine. The induction generator, soft starter, the capacitor bank for reactive power compensation and the step-up transformer are all placed in the nacelle, and thus the transformer is considered part of the wind turbine. The control of active and reactive power is based on measured power at the Main Switch Point MSP.

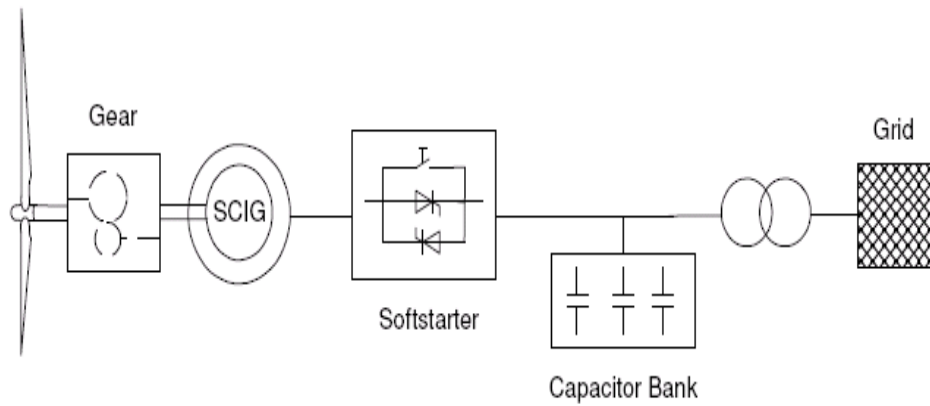


**Figure 6: Active stall wind turbine layout including softstarter and capacitor bank.**

### 3.1.1 Active stall wind turbine control during normal operation

Wind turbine controller must be able to adjust the wind turbine production to the power reference demanded by the system operator. In case of normal operation conditions, the wind turbine has to produce maximum power. In power limitation operation mode, the wind turbine has to limit its production to the power reference received from a wind farm controller or directly from the system operator. The power reference required from the wind turbine can be equal to the rated power of the wind turbine or less than that. Figure 7 illustrates the power curve and  $C_p$  curves for a 2 MW active stall wind turbine for different imposed power setpoints.

Notice that by imposing a power set point lower than the designed rated power of the wind turbine, the wind turbine range with high aerodynamic efficiency is, as expected,

reduced, while the maximum aerodynamic efficiency is moving toward lower wind speeds.

The model described in [16] is a traditional power controller designed for a typical active stall wind turbine. This traditional controller is very slow because it tries to reduce the pitch activity as much as possible to limit the stress of the pitch system. Such a controller design is not optimal for grid support, since in this case the wind turbine or the wind farm is asked to act as a fast active element in the power system. To speed up the power control, a new active stall power controller is proposed and described in this chapter. To provide the best grid support, the aim is to use a simpler power controller, which enables fast control of the wind turbine power to different power setpoints imposed for example by system operator.

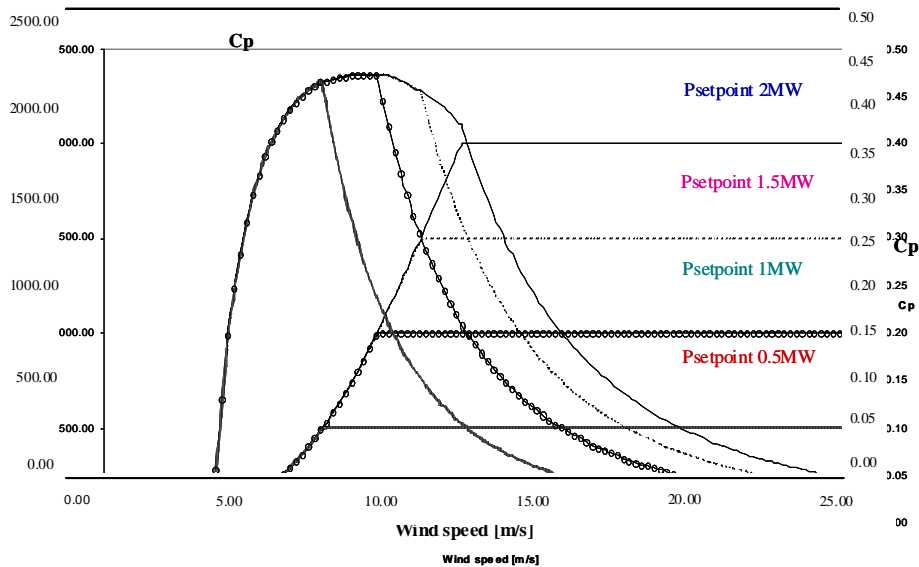


**Figure 7: Power curve and Cp curve for different wind turbine power setpoints.**

Figure 8 illustrates the power control scheme for an active stall wind turbine described in [10]. A PI controller with antiwind-up ensures a correct active power production from the wind turbine both in power optimization control and power limitation control modes. The input of the controller is the error signal between the measured active power at the Main Switch Point (MSP) and an imposed active power reference. The PI controller produces the pitch angle reference  $\theta_{ref}$ , which is further compared to the actual pitch angle  $\theta$  and then the error  $\Delta\theta$  is corrected by the servomechanism. In order to get a

realistic response in the pitch angle control system, the servomechanism model accounts for a servo time constant  $T_{servo}$  and the limitation of both the pitch angle and its gradient. The output of the actuator is the actual pitch angle of the blades.

The available power of the wind turbine can be monitored at each instant, based on the wind turbine's power curve and the filtered wind speed  $u_f$ , as illustrated in Figure 8. The

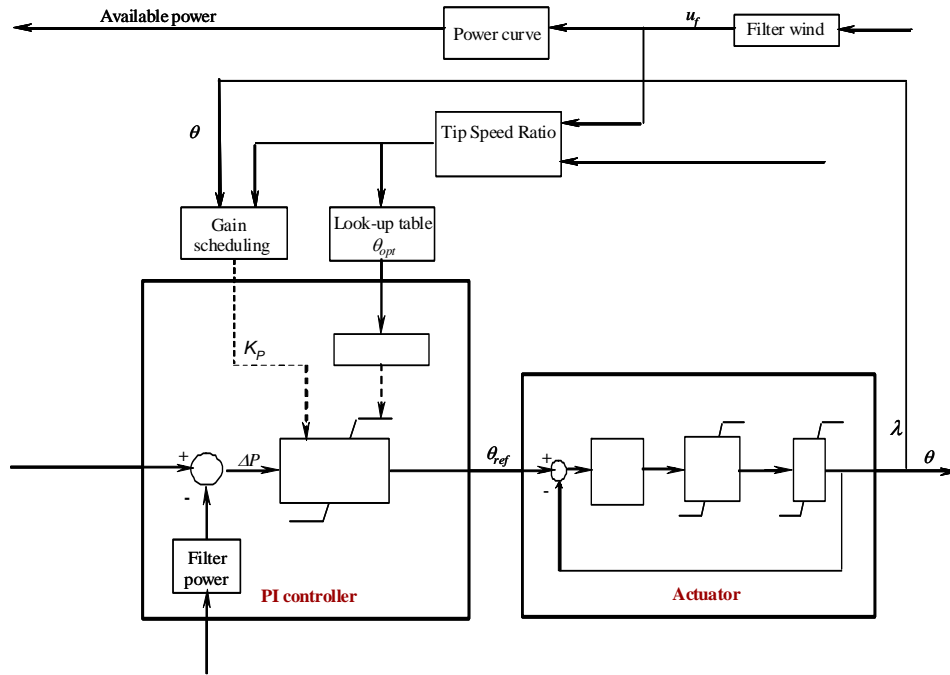


Figure 8: Grid support active power control scheme.

wind speed is filtered appropriately to avoid unnecessary fluctuations.

In the power optimization control mode, the controller has to maximize the power production. In this case the difference between the measured power and its reference value is always positive and is integrated up until the pitch reference angle reaches the upper limit of the controller. The optimal pitch angle is thus given by the upper limitation of the controller. This upper limitation is calculated on-line based on an “optimal pitch” look-up table as a function of the estimated tip speed ratio  $\lambda = \omega_{WTR} R / u_f$ , where  $\omega_{WTR}$  is the wind turbine rotor speed,  $R$  is the rotor radius and  $u_f$  is the filtered wind speed.

In the power limitation control mode the error signal  $\Delta P$  of the controller is negative and therefore the pitch angle moves from the upper limitation and starts to actively drive

the measured power to the power reference. Notice that the measured power used in the error signal is low pass filtered in order to avoid the 3p fluctuations (three times the rotational frequency) in the power causing the pitch angle to fluctuate with the 3p frequency as well. This is because it is assumed that the pitch system is too slow to remove the 3p from the power, and thus the 3p fluctuations in the power would stress the system unnecessarily.

Compared with the controller presented in [16], the controller presented in [10] contains an additional gain scheduling control of the pitch angle in order to compensate for the existing non-linear aerodynamic characteristics. The gain scheduling is necessary to ensure that the total gain of the system remains unchanged irrespective of the operational point of the wind turbine. The non-linear aerodynamic characteristics imply that the effect of pitching on the power varies depending on the operational point. The goal of the gain scheduling is therefore to change the proportional gain of the controller  $K_p$  in such a way that the total gain of the system remains unchanged irrespective of the operational point of the wind turbine. The pitch sensitivity, namely the effect of pitching, can be expressed mathematically by  $\frac{dP}{d\theta}$ . The total gain  $K_{system}$  of the system can be then expressed as the proportional gain of the PI controller,  $K_p$ , times the pitch sensitivity of the system  $\frac{dP}{d\theta}$ , as follows:

$$K_{system} = K_p \frac{dP}{d\theta} = K_0 \left[ \frac{dP}{d\theta} \right]^{-1} \frac{dP}{d\theta} = const. \quad (6)$$

where  $K_0$  is a dimensionless constant independent of the operation point.

The total gain of the system  $K_{system}$  is kept constant by changing  $K_p$  in such a way that it counteracts the variation of the pitch sensitivity  $\frac{dP}{d\theta}$  by the reciprocal sensitivity function  $\left[ \frac{dP}{d\theta} \right]^{-1}$ , hence:

$$K_p = K_0 \left[ \frac{dP}{d\theta} \right]^{-1} \quad (7)$$

The pitch sensitivity  $\frac{dP}{d\theta}$  of the system depends on the operational point of the wind turbine. The operation point of the wind turbine is characterized directly by the wind speed and the power set point and indirectly by the pitch angle and tip speed ratio. The implementation of the gain scheduling, namely the expression of the non-linear aerodynamic amplification in the system, is performed on-line based on the simulated pitch angle and tip speed ratio, according to:

$$\frac{dP}{d\theta} = \frac{1}{2} \rho \pi R^2 u_f^3 \frac{dC_p}{d\theta} \quad (8)$$

where  $u_f$  is the filtered wind speed and the power coefficient  $C_p = C_p(\theta, \lambda)$  depends on the pitch angle  $\theta$  and the tip speed ratio  $\lambda$ . Figure 9 illustrates the pitch sensitivity for different wind speeds and power set points.

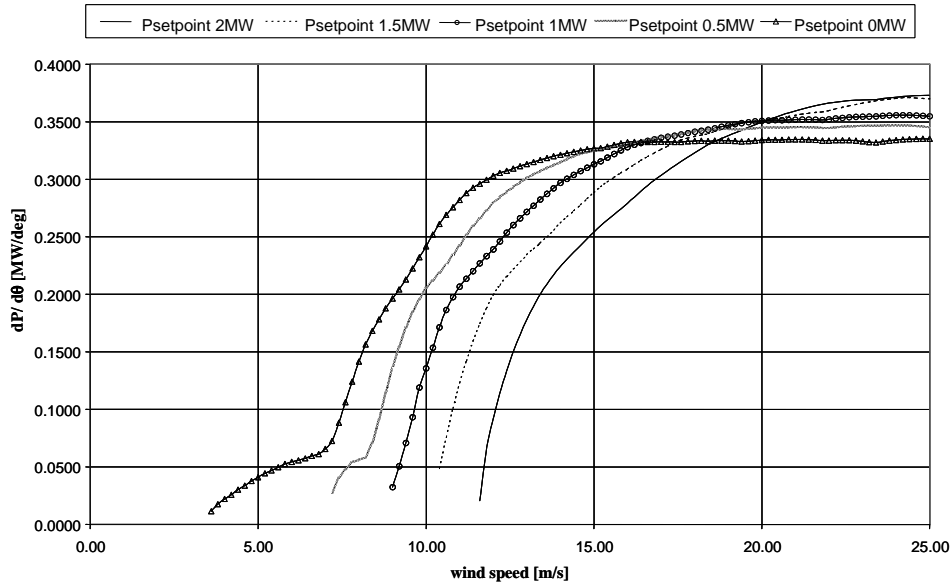


**Figure 9: Pitch sensitivity function versus wind speed for different power set points.**

Notice that the pitch sensitivity increases at higher wind speeds. This shows that the more sensitive the system is (larger pitch angles  $\theta$  / higher wind speeds) the smaller the



gain for the controller should be and vice versa. When the active power set point is decreased, the pitch sensitivity becomes significant also for lower wind speeds.

### 3.1.2 Active stall wind turbine control during grid faults

The fault ride-through capability of an ASIG wind farm, and thus its stabilization at a short circuit fault, can be achieved by reducing the wind turbine power production for duration of few seconds from the moment of fault occurrence.

In this work, the ASIG wind turbine control strategy during grid faults is implemented based on [17]. The idea is that during the fault, the ASIG wind turbine normal controller, illustrated in Figure 8 is switched off and replaced by a control strategy to reduce directly the mechanical power of the rotor to a predefined level. The ordering of power reduction is given for example when the monitoring of the grid voltage indicates a fault occurrence. When the grid fault is cleared, the wind turbine continues running at reduced power for still few seconds, after which it starts to ramp up the mechanical power of the rotor and re-establish the control for ASIG wind turbine normal operation conditions.

### 3.1.3 Active stall wind turbine grid support

Compared with the controller described in [16], the wind turbine controller presented in [10] contains also an additional controller for the reactive power of the wind turbine. As illustrated in Figure 6, a capacitor bank is chosen to compensate for the reactive power absorbed by the induction generator or required by the grid operator. The reactive power consumption of an induction generator is a function of its loading and it increases as the active power increases. The power factor of the induction generator at rated load is usually in the range of 0.85-0.90, which means that the consumption of reactive power is typically about half of the active power generation. This aspect is taken into account in the design of the size of the capacitor bank. In order to be able to produce reactive power to the grid, the size of capacitor bank should thus be larger than the amount of reactive power consumed by the generator.

In the present implementation, a standard DIgSILENT SVC component is used to model the capacitor bank instead of a number of individual capacitors as used in earlier models [12]. The SVC component is a standard component in DIgSILENT and has the

advantage of being an effective and easier way to simulate a capacitor bank consisting of several capacitor steps of the same size.

The standard SVC component is a combination of a shunt capacitor bank and a thyristor controlled reactance (TCR). The thyristor controlled reactance is usually used for a continuous control of reactive power. However, the compensation unit in wind turbines consists only of capacitors. Thus the TCR part of the standard SVC component is deactivated in the design of the present SVC control.

A discrete control of SVC is implemented using the dynamic simulation language DSL of DIgSILENT – see Figure 10. The capacitors in the capacitor bank can be switched on and off individually by the control system, depending on the load situation, in response to changes in the reactive power demand.

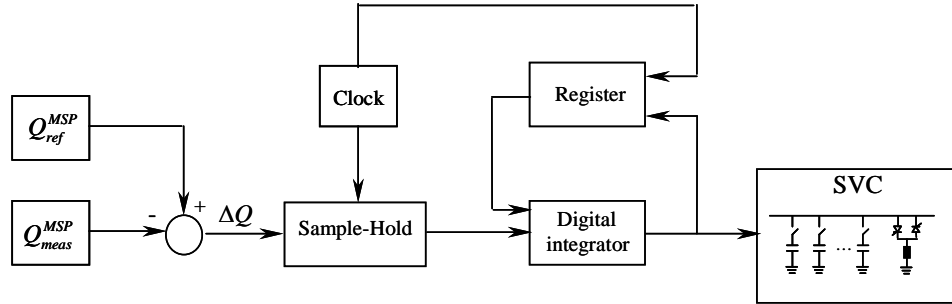


**Figure 10: Designed SVC control for the active stall wind turbine.**

The difference  $\Delta Q$  between the measured reactive power  $Q_{meas}^{MSP}$  on the low voltage side of the step-up transformer at the Main Switch Point MSP (see Figure 10) and an imposed reference reactive power  $Q_{ref}^{MSP}$ , is used inside a sample-and-hold block. This block stores its sampled input signal at the output until the next rising edge of the clock signal appears. The clock supervises furthermore a register, which memorizes the number of capacitors, which have been switched on at the previous clock period. For each clock period, based on the new updated and the old loading situation, a digital integrator determines the required number of capacitors.

The control system of SVC has to solve a dilemma: it must be able to switch the capacitors fast in order to be able to support the grid but on the other hand it should not attempt to control the 3p fluctuations in the reactive power consumption of the induction generator due to the wind fluctuations. The traditional wind turbines with directly connected induction generators are equipped with standard capacitor banks using

mechanical contactors, which are typically controlled in intervals of 1-10 minutes. This control is not fast enough in the case when the turbine has to support the grid. However, if the capacitors are switched more often using mechanical contactors, the transients due to the switchings will reduce the lifetime of the capacitors and contactors too much. To provide a faster control possibility, new wind turbines are using thyristor switches instead of mechanical contactors, which can reduce the switching transients significantly and thus make it possible to switch the capacitor much more often without reducing the lifetime significantly.

As an example, the active stall controlled Bonus wind turbines in Nysted offshore wind farm in Denmark are equipped with such a dynamic phase compensation unit, using thyristor switches. Another similar dynamic phase compensation unit was tested on a wind turbine by Sørensen et.al.[18]. This test concluded that the dynamic phase compensation technology should not be used to remove the 3p fluctuations in reactive power, because the transients caused by the many capacitor switchings appeared to cause more flicker than could be removed by dynamically compensating the 3p reactive power fluctuations.

The control system of the capacitor bank has thus to switch the capacitors fast in order to be able to support the grid, but on the other hand it should not attempt to control the 3p fluctuations in the reactive power consumption of the induction generator.

In the present work, the fast switching of the capacitors is ensured by the clock time 20 ms, while the insensitivity to 3p fluctuations in the wind speed is realized by implementing a hysteresis in the digital integrator. The output of the digital integrator is sent directly to the SVC component and thus the required number of capacitors is switched on or off. The hysteresis has been used instead for a low pass filter in order to keep a very fast response to large changes in the reactive power reference. This is regarded as important for the ability of the wind turbines to support with voltage control.

### **3.2 Doubly-fed induction generator wind turbine**

A DFIG system is essentially a wound rotor induction generator with slip rings, with the stator directly connected to the grid and with the rotor interfaced through a back-to-back partial-scale power converter. The DFIG is doubly fed by means that the voltage on the

stator is applied from the grid and the voltage on the rotor is induced by the power converter. The converter consists of two conventional voltage source converters (rotor-side converter RSC and grid-side converter GSC) and a common dc-bus, as illustrated in Figure 11.

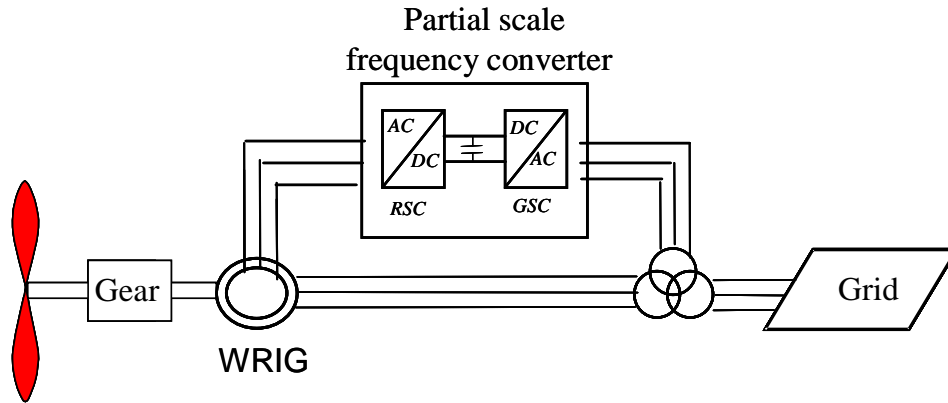


**Figure 11: DFIG wind turbine configuration.**

The objective of the rotor side converter (RSC) is to control independently the active power of the generator and the reactive power produced or absorbed from the grid. The objective of the grid side converter (GRC) is to keep the dc-link voltage constant regardless of the magnitude and the direction of the rotor power and to guarantee a converter operation with unity power factor (zero reactive power). This means that the grid side converter exchanges only active power with the grid, and therefore the transmission of reactive power from DFIG to the grid is done only through the stator [19]. The behavior of the generator is governed by these converters and their controllers both in normal and fault conditions.

### 3.2.1 DFIG wind turbine control during normal operation

Figure 12 sketches the overall control system of a variable speed DFIG wind turbine implemented in DIgSILENT. Two control levels using different bandwidths can be distinguished:

- Doubly-fed induction generator (DFIG) control level
- Wind turbine control level

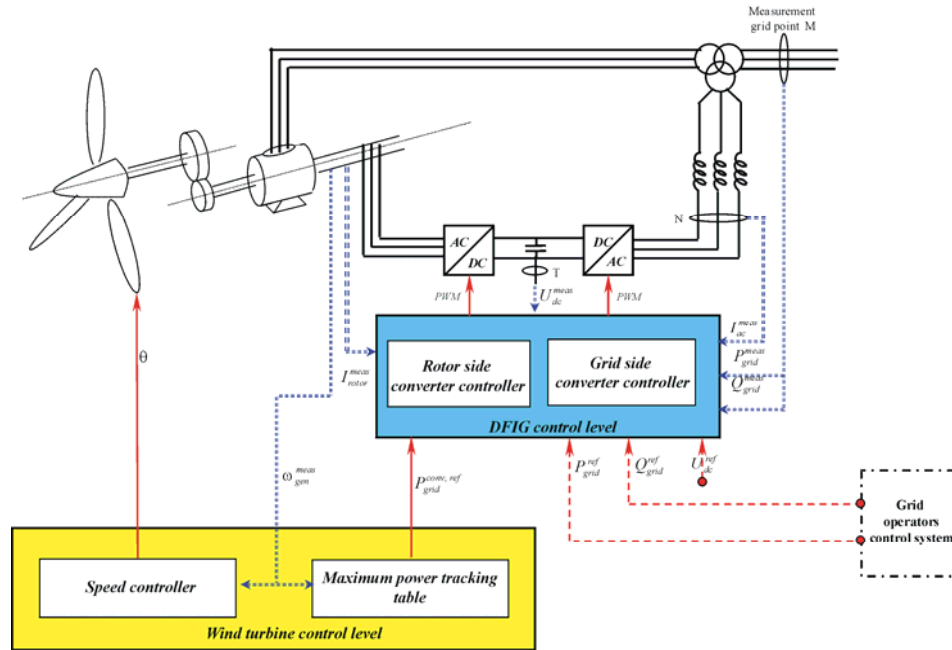


**Figure 12: Overall control system of variable speed wind turbine with doubly-fed induction generator.**

The DFIG control, with a fast dynamic response, contains the electrical control of the power converters and of the doubly-fed induction generator. The DFIG control contains the controllers of the rotor side converter and grid side converter.

The wind turbine control, with slow dynamic response, provides reference signals both to the pitch system of the wind turbine and to the DFIG control level. It contains two controllers:

- Speed controller - has as task to control the generator speed at high wind speeds i.e. to change the pitch angle in order to prevent the generator speed becoming too. At low wind speeds, the pitch angle is kept constant to an optimal value. A gain scheduling control of the pitch angle is implemented in order to compensate for the existing non-linear aerodynamic characteristics.
- Maximum power tracking controller – generates the active power reference signal for the active power control loop, performed by the rotor side converter controller in DFIG control level. This reference signal is determined from the predefined characteristic  $P - \omega$  look-up table, illustrated in Figure 13, based on filtered measured generator speed. This characteristic

is based on aerodynamic data of the wind turbine's rotor and its points correspond to the maximum aerodynamic efficiency.

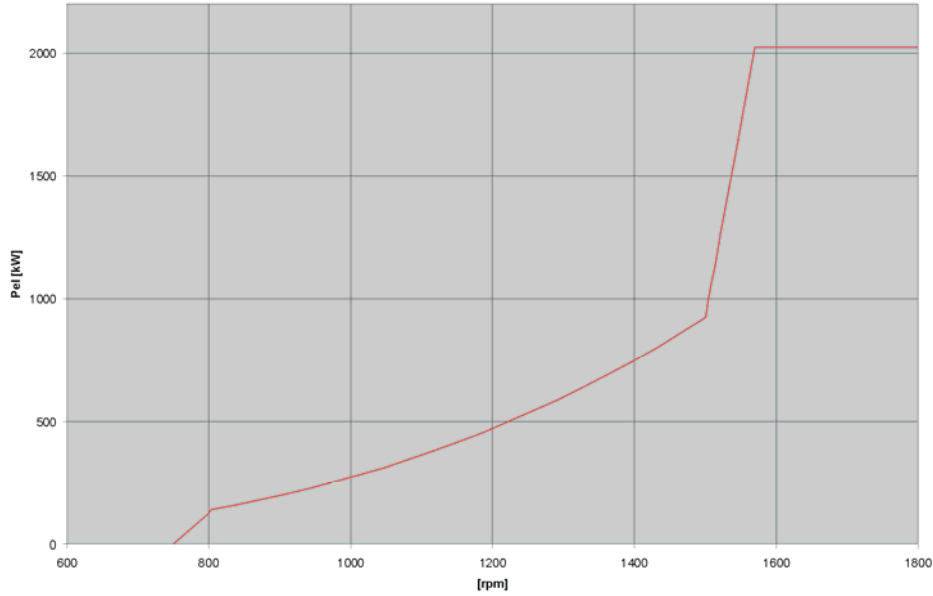


**Figure 13: Power-omega characteristic used in the maximum power-tracking controller.**

Both the speed controller and the maximum power-tracking controller are active in the power limitation strategy, while only maximum power tracking controller is active in the optimization power strategy. In the case of high wind speeds there is a cross coupling between these two controllers.

Figure 14 illustrates explicitly the speed controller, the maximum power tracking controller and the rotor side converter controller. The grid side converter controller does not interact directly with the wind turbine controller, and therefore it is shown as a “black box”.

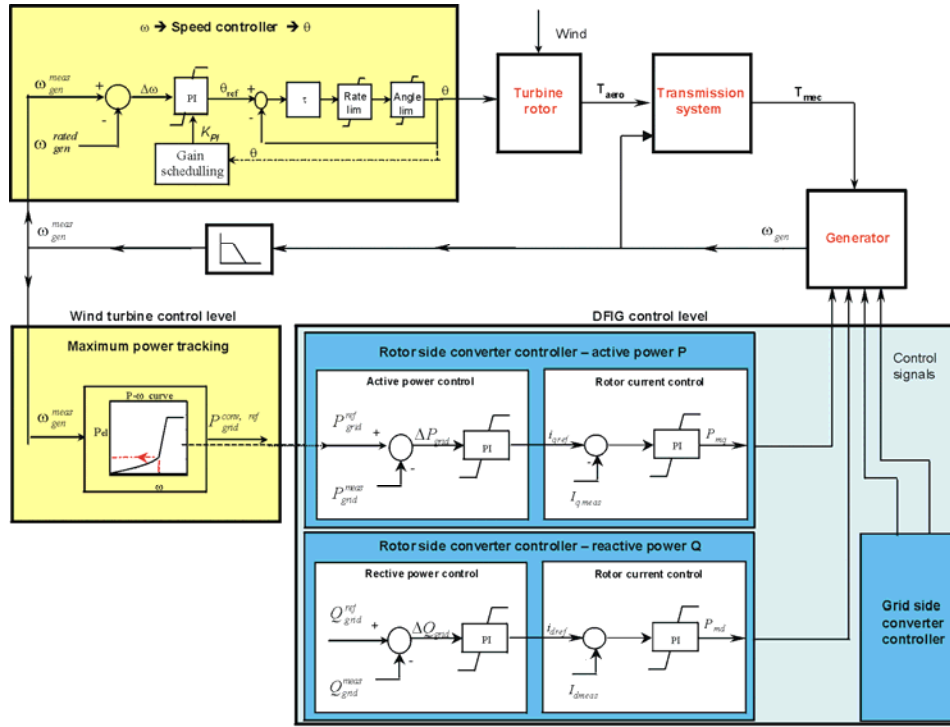


**Figure 14: DFIG wind turbine control during normal operation.**

In the rotor side converter control, there are two independent control branches, one for the active power control and the other for reactive power control. Each branch consists of 2 controllers in cascade.

Notice that all these controllers, except maximum power tracking controller, are basically PI controllers. Both the speed controller and the maximum power tracking have as input the filtered measured generator speed. The generator speed is measured and a low-pass filter is used to avoid that the free-free frequency in the transmission system is amplified through the control system.

The DFIG control structure, illustrated in Figure 14, contains the electrical control of the power converters, which is essential for the DFIG wind turbine behavior both in normal operation and during fault conditions.

Power converters are usually controlled utilizing vector control techniques [20], which allow de-coupled control of both active and reactive power. The aim of the RSC is to control independently the active and reactive power on the grid, while the GSC has to keep the dc-link capacitor voltage at a set value regardless of the magnitude and the direction of the rotor power and to guarantee a converter operation with unity power

factor (zero reactive power). As illustrated in Figure 14, both RSC and GSC are controlled by a two stage controller. The first stage consists of very fast current controllers regulating the rotor currents to reference values that are specified by a slower power controller (second stage).

The control performance of the DFIG is very good in normal grid conditions. DFIG control can, within limits, hold the electrical power constant in spite of fluctuating wind, storing thus temporarily the rapid fluctuations in power as kinetic energy.

The active and reactive power set-point signals for the second stage controllers of the converters in Figure 14 are depending on the wind turbine operational mode (normal or fault operation) signals. For example, in normal operation:

The active power set-point  $P_{ref}^{grid}$  for the rotor-side converter is defined by the maximum power tracking point (MPT) look-up table. The reactive power set-point  $Q_{ref}^{grid}$  for the rotor-side converter can be set to a certain value or to zero according to whether or not the DFIG is required to contribute with reactive power.

The grid-side converter is reactive neutral (i.e.  $Q_{ref}^{GSC}=0$ ) in normal operation. This means that, in normal operation, the GSC exchanges with the grid only active power, and therefore the transmission of reactive power from DFIG to the grid is done only through the stator. The dc-voltage set-point signal  $U_{dc}$  is set to a constant value, independent on the wind turbine operation mode.

The use of the partial-scale converter to the generator's rotor makes DFIG concept on one hand attractive from an economical point of view. On the other hand, this converter arrangement requires advanced protection system, as it is very sensitive to disturbances on the grid.

### 3.2.2 DFIG wind turbine control during grid fault operation

The grid fault is affecting both the mechanical and the electrical part of the wind turbine. During a grid fault, voltage and power at the wind turbine terminal drop and thus the power in the DFIG drops, too. This results in an acceleration of turbine and generator, which is counteracted by the speed controller, i.e. by the pitch angle control, which thus



serves as an over speed protection. Moreover, when the electrical power drops the drive train will start to oscillate.

During grid faults, the electrical torque is significantly reduced, and therefore the drive train system acts like a torsion spring that gets untwisted. Due to the torsion spring characteristic of the drive train, the mechanical torque, the aerodynamical torque and thus the generator speed start to oscillate with the so-called free-free frequency:

$$f_{osc} = \frac{1}{2\pi} \cdot \sqrt{\frac{k}{J_{eq}}}$$

where  $J_{eq}$  is the equivalent inertia of the drive train model, determined by:

$$J_{eq} = \frac{J_{rot} \cdot n_{gear}^2 \cdot J_{gen}}{J_{rot} + n_{gear}^2 \cdot J_{gen}}$$

As these torsional oscillations may influence the converter operation both during grid faults and a short while after the grid faults have been removed, their modeling by using at least a two-mass model for the drive train system is essential. Furthermore, these torsional oscillations can even be excited and become undamped at a fast converter control [21]. Due to this reason a damping controller is implemented as shown in Figure 15, which actively damps any torsional oscillations of the drive train and prevents instability of the system and substantially reduces the mechanical stresses of the turbine.

Without any protection system, the concern in DFIG is usually the fact that large grid disturbances can lead to large fault currents in the stator due to the stator's direct connection to the grid. Because of the magnetic coupling between the stator and the rotor and of the laws of flux conservation, the stator disturbance is further transmitted to the rotor. High voltages are thus induced in the rotor windings that on their turn cause excessive currents in the rotor as well. Furthermore, the surge following the fault includes a “rush” of power from the rotor terminals towards the converter.

Since the stator-rotor ratio of the DFIG is designed according to the desired variable speed range, in the case of grid faults it might not be possible to achieve the desired rotor voltage in order to control the high rotor currents. This means that the converter reaches fast its limits and as a consequence, it loses the control of the generator during the grid fault [6]. As the grid voltage drops in the fault moment, the GSC is not able to transfer

the power from the RSC further to the grid and therefore the additional energy goes into charging the dc bus capacitor, i.e. dc bus voltage rises rapidly.

A protection system of the DFIG converter is thus necessary to break the high currents and the uncontrollable energy flow through the RSC to the dc-link and thus to minimize the effects of possible abnormal operating conditions. The protection system monitors usually different signals, such as the rotor current, the dc-link voltage and when at least one of the monitored signals exceeds its respective relay settings, the protection is activated.

A simple protection method of the DFIG under grid faults is to short circuit the rotor through a device called crowbar. The crowbar protection is external rotor impedance, coupled via the slip rings to the generator rotor instead of the converter. The function of the crowbar is to limit the rotor current.

When the crowbar is triggered, the rotor is short circuited over the crowbar impedance, the rotor-side converter (RSC) is disabled and therefore the DFIG behaves as a conventional squirrel cage induction generator (SCIG) with an increased rotor resistance. The independent controllability of active and reactive power gets thus unfortunately lost. Since the grid-side converter (GSC) is not directly coupled to the generator windings, there is no need to disable this converter, too. The GSC can therefore be used as a STATCOM to produce reactive power (limited however by its rating) during grid faults.

An increased crowbar resistance improves the torque characteristic and reduces the reactive power demand of the generator at a certain speed [22]. By the addition of the external resistance (crowbar resistance) in the rotor circuit during grid faults, the pull-out torque of the SCIG generator is moved into the range of higher speeds. The dynamic stability of the SCIG generator is thus improved by increasing the external resistance [21].

In normal operation the active power set-point  $P_{ref}^{grid}$  for the RSC control is defined by the maximum power tracking point (MPT) look-up table, as function of the optimal generator speed – see Figure 15. This means that for each wind speed there is only one generator speed resulting in maximum aerodynamic coefficient  $C_p$ . However, in case of

grid faults, the generator speed variation is not due to the wind speed change but due to electrical torque reduction. This means that, in the case of grid faults the active power set-point  $P_{ref}^{grid}$  has to be differently defined, i.e. as the output of a damping controller. Such a controller has as task to damp the torsional excitations which are excited in the drive train owing to the grid fault.

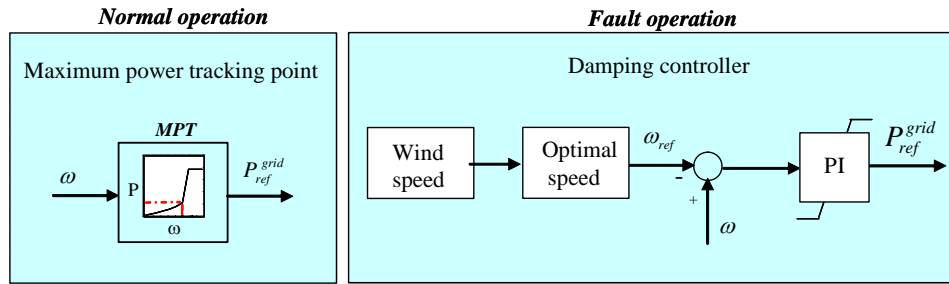


**Figure 15: Definition of active power set-point for normal and fault operation, using MPT and damping controller respectively.**

Different control schemes can be applied to damp these torsional oscillations. In this work, the damping controller suggested by [21] is adopted. As illustrated in Figure 15, the PI damping controller produces the active power reference signal  $P_{ref}^{grid}$  based on the deviation between the actual generator speed and its reference. The speed reference is defined by the optimal speed curve at the incoming wind. The damping controller is tuned to actively damp the torsional oscillations excited at a grid fault in the drive train system. [22] shows that absence or insufficient tuning of this PI controller may lead to self-excitation of the drive train system and to a risk of tripping as protection against vibrations in the mechanical construction.

The pitch control system is not able to damp the torsional oscillations, because of several delay mechanisms in the pitch [23]. The pitch control damps the slow frequency variations in the generator speed, while the damping controller is able to damp the fast oscillations in the generator speed.

During a grid fault, the tasks of RSC and GSC can be changed, depending on whether the protection system (i.e. crowbar) is triggered or not. In the case of less severe grid faults (i.e. not triggered crowbar) or reactive power unbalance in the system, the RSC and the GSC have the same tasks as in normal operation. In the case of severe fault

(i.e. triggered crowbar), a specific grid support strategy has to be designed and developed.

### 3.2.3 DFIG wind turbine grid support

The technical specifications for the wind turbines, as defined by the power system operator, require wind turbines to behave as active components and to support the grid. In this report, the attention is mainly drawn to the DFIG voltage grid support during grid faults.

In general, different possible voltage control strategies exist for regulating voltage at the terminals of DFIG wind turbines. The voltage can in principle be controlled by either the RSC [24] or the GSC [25] or by both of them [21]. There is limited information in the literature about the latter voltage control method. The attention in this report is therefore drawn to the voltage control strategy, where the reactive power contribution is performed by both converters in a co-ordinated manner. The idea is that the RSC is used as default reactive power source, while the GSC is used as a supplementary reactive power source during the blocking of the RSC.

At a severe grid fault, if the generator is not tripped, the DFIG wind turbine has to continue its operation with a short circuited generator, trying to sustain grid connection. When the crowbar is triggered, the RSC is blocked. In such situation, the RSC's controllability is lost and the DFIG grid support capability is thus strongly reduced. A solution to enhance the DFIG grid support capability during grid faults is to design a control strategy where the grid voltage (reactive power) control is taken over by the GSC. The GSC does not block at a grid fault, but it continues its operation as STATCOM as long as the RSC is blocked. When the crowbar is removed, the RSC starts to operate and the GSC is set again to be reactive neutral. The removal of the crowbar protection, and thus the re-start of the RSC can be performed according to different criteria, such as the magnitude of the grid voltage or of the rotor currents. A too soon RSC restarting may cause tripping of the converter again at the fault clearance.

As illustrated in Figure 16, the DFIG voltage grid support strategy is implemented in this work as an extension of the DFIG control structure used in normal operation and presented in Figure 14.

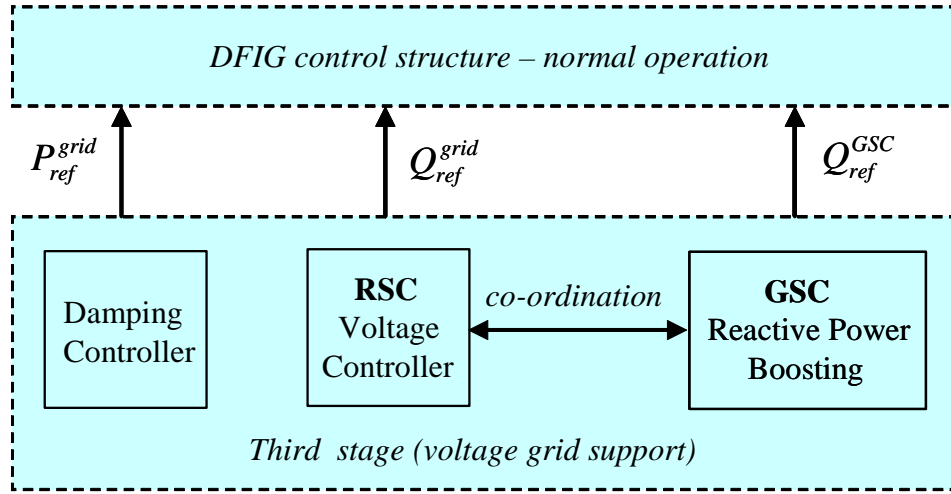


**Figure 16: Extended DFIG control structure for voltage grid support during grid faults.**

An additional third control stage, having as task to improve the DFIG voltage grid support capability during grid fault, is thus added to the DFIG control structure used in normal operation [6]. This third (voltage) control stage, used in the case of fault operation and illustrated in Figure 16, provides the reference signals for the second stage controllers. This control stage contains three controllers, such as a damping controller, a rotor-side converter (RSC) voltage controller and a grid-side converter (GSC) reactive power boosting.

The damping controller, illustrated in Figure 15, is attenuating the oscillations in the drive train produced by the grid fault. It ensures the fault ride-through capability of the wind turbine, i.e. avoids an eventual wind turbine grid disconnection due to undamped oscillations in the generator speed. The RSC voltage controller controls the grid voltage as long as the RSC is not blocked.

The GSC reactive power boosting (a supplementary reactive power controller) generates a reactive power reference signal  $Q_{ref}^{GSC}$  for the GSC voltage control, in the case when RSC is blocked. The implemented reactive power boosting provides a zero reactive power reference when the RSC is active, and a maximum reactive power of the GSC (1p.u.) as reference value in the case when the RSC is blocked. This means that the GSC contributes with its maximum reactive power capacity for grid support under severe grid faults.

As illustrated in Figure 16, a co-ordination between the RSC and GSC voltage control is implemented. During the grid fault, some of the controllers have to be disabled, while others are enabled. The enabling (start-up) of the controllers requires to be treated with some care to avoid discontinuities and to minimize the loads on wind turbines. Such discontinuities could eventually lead to prolonged transients and, implicitly, to subsequent operations of the crowbar protection.

### 3.3 Multi-pole PMSG wind turbine grid support

A typical configuration of a variable speed wind turbine based on a multi-pole permanent magnet synchronous generator (PMSG) is illustrated in Figure 17. It consists of:

- Wind turbine mechanical level:
  - Aerodynamics
  - Gearless drive train
  - Pitch angle control
- Wind turbine electrical level:
  - Multi-pole permanent magnet synchronous generator (PMSG)
  - Full-scale frequency converter and its control

In this configuration, the synchronous generator is connected to the grid through a full-scale frequency converter system that controls the speed of the generator and the power flow to the grid. The full-scale frequency converter system consists of a back-to-back voltage source converter (generator-side converter and the grid-side converter connected through a DC link), controlled by IGBT switches. The rating of the converter system in this topology corresponds to the rated power of the generator plus losses. The use of such a converter enables the PMSG to keep its terminal voltage on a desired level and to adjust its electric frequency according to the optimized mechanical frequency of the aerodynamic rotor, independently of the fixed electric frequency and the voltage of the AC grid. The electric frequency  $f_e$  at the PMSG terminals is the product of the mechanical frequency  $f_m$  of the wind turbine rotor and the number of generator pole-pairs  $p$ :

$$f_e = f_m p \quad [Hz] \quad (9)$$

where the mechanical frequency  $f_m$  of the generator rotor is related to the turbine rotor speed  $\omega_m$ :

$$\omega_m = 60 f_m \quad [rpm] \quad (10)$$

As illustrated in Figure 17, the aerodynamic rotor of the wind turbine is directly coupled to the generator without any gearbox, i.e. through a gearless drive train. The permanent magnets are mounted on the generator rotor, providing a fixed excitation to the generator. The generator power is fed via the stator windings into the full-scale frequency converter, which converts the varying generator frequency to the constant grid frequency.

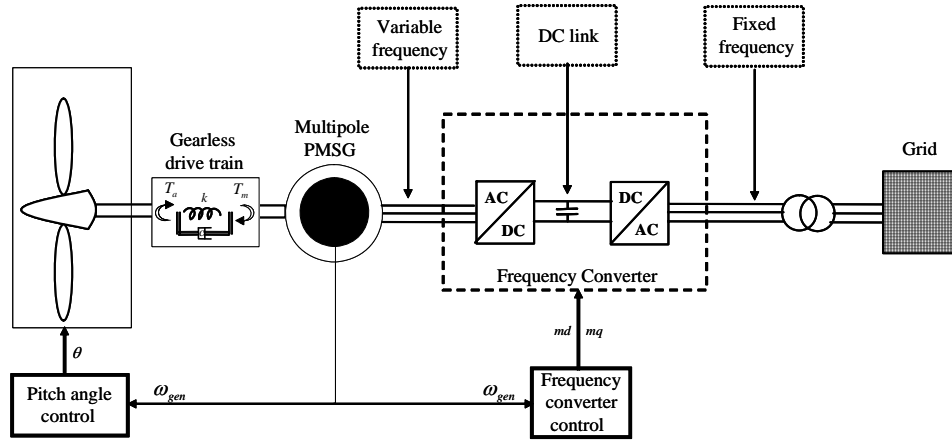


Figure 17: Variable speed multi-pole PMSG wind turbine configuration.

### 3.3.1 PMSG wind turbine control during normal operation

The control system consists of two co-ordinated controllers: the wind turbine controller, i.e. pitch angle controller, and the frequency converter controller. Both controllers are using information about the generator speed. Contrarily fixed speed wind turbines, where the power flow to the grid is dependent on the aerodynamical power that drives the wind turbine, in variable speed wind turbines the power flow to the grid and thus the generator speed are controlled by the frequency converter according to an optimal power characteristic. The pitch controller controls the generator speed as well, but it is operational only at high wind speeds.

Since the PMSG is connected to the grid through the back-to-back converter, only the active power of the PMSG is transferred to the grid. The reactive power cannot be exchanged through the DC link in the converter system. However, the grid-side converter, whose electric frequency and voltage are fixed to the grid, can be set to control the reactive power/voltage on the grid.

The pitch angle control is realised by a PI controller with antiwind-up, using a servomechanism model with limitation of both the pitch angle and its rate-of-change, as illustrated in Figure 18. The pitch angle controls the generator speed, i.e. the input in the controller is the error signal between the measured generator speed and the reference generator speed. The pitch angle controller limits the rotor speed when the nominal generator power has been reached, by limiting the mechanical power extracted from the wind and thus restoring the balance between electrical and mechanical power. A gain scheduling control of the pitch angle is implemented in order to compensate for the nonlinear aerodynamic characteristics [26].

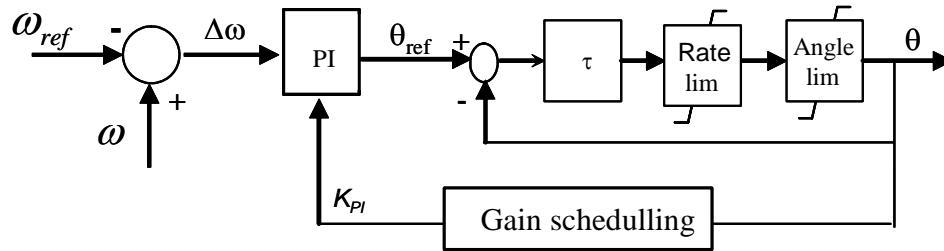


**Figure 18: Pitch angle control.**

Similar to DFIG wind turbines, the PMSG wind turbines behavior is strongly dependent on the frequency converter control both in normal and fault operation conditions.

Frequency converters are usually controlled utilizing vector control techniques [20]. Briefly, vector control allows decoupled control of both active and reactive power. The idea is to use a rotating reference frame based on an AC flux or voltage and then to project currents on this rotating frame. Such projections are usually referred to as the d and q components of their respective currents. With a suitable choice of reference frames the AC currents appear as DC quantities in the steady state. For flux-based rotating frames, changes in the q component will lead to active power changes, while changes in



the d component will lead to reactive power changes. In voltage-based rotating frames (and thus 90° ahead of flux-based frames) the effect is the opposite.

The control of the converter can be realized using different strategies:

- The generator-side converter controls traditionally the active power flow  $P_{\text{grid}}$  to the grid. Besides this, it has also to control the generator reactive power  $Q_{\text{gen}}$  or the generator stator voltage  $U_s$ . However, instead of the active power flow  $P_{\text{grid}}$ , the generator-side converter can also control the DC-link voltage  $U_{\text{DC}}$ . The control of the active power and of the DC-link voltage is strongly related to each other, as the active power can be fed into the grid as long as the DC-link voltage is kept constant.
- The grid-side converter controls typically the DC-link voltage  $U_{\text{DC}}$  as well as the reactive power flow  $Q_{\text{grid}}$  to the grid. Again, instead of the DC-link voltage  $U_{\text{DC}}$ , the grid-side converter can also control the active power flow  $P_{\text{grid}}$  to the grid.

In this investigation, the proposed full-scale converter control is modeled on a generic level, without focusing on any particular design of a manufacturer. As illustrated in Figure 19, the control uses an AC voltage oriented reference frame, i.e. d-axis to control the active current, while q-axis to control the reactive current.

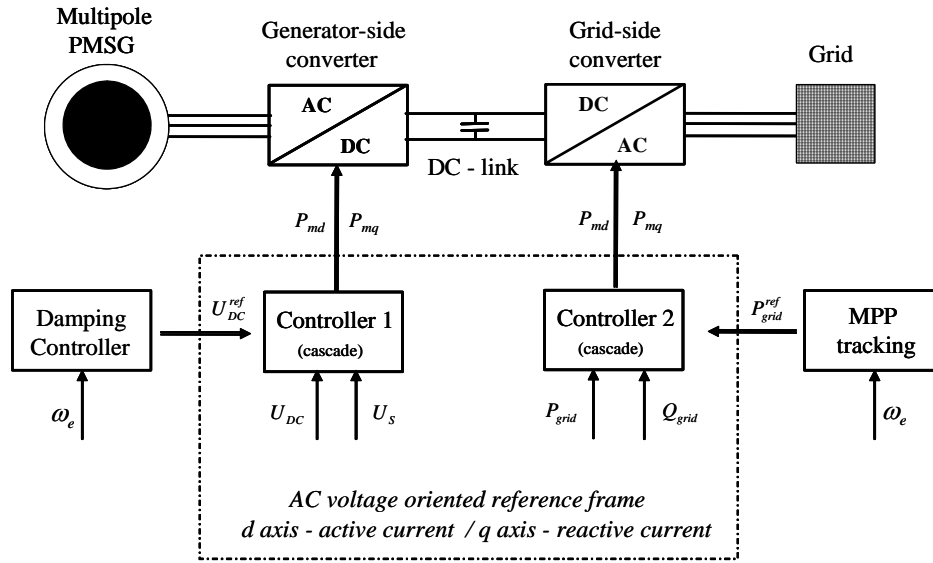


**Figure 19: Power converter control strategy of the variable speed multi-pole PMSG wind turbine.**

It consists of the following controllers:

- Damping controller:
  - Ensures a stable operation of the wind turbine, by damping the torsional oscillations excited in the drive train and reflected in the generator speed  $\omega_e$ .
- Generator-side converter controller (controller 1):
  - Keeps constant the DC-link voltage  $U_{DC}$  and controls the generator stator voltage  $U_s$  to its rated value in the stator voltage reference frame. The advantage of controlling the generator stator voltage  $U_s$  to its rated value is that the generator and the power converter always operate at the rated voltage, for which they are designed and optimized.
- Grid-side converter controller (controller 2):
  - Controls independently the active  $P_{grid}$  and the reactive  $Q_{grid}$  power to the grid in the grid voltage reference frame

Similar to the control of DFIG wind turbines [26], the control of the generator-side converter and the grid-side converter in variable speed multi-pole PMSG wind turbines is

also based on two control loops in cascade: a very fast inner current controller regulating the currents to the reference values that are specified by the outer slower power controller. The current controller provides reference signals in d- and q- axis ( $P_{md}$  and  $P_{mq}$ ) for the PWM-controlled power converter.

The reason of using a damping controller is due to the fact that a multi-pole PMSG wind turbine with full-scale converter has no inherent damping. This implies that any small speed oscillation excited by mechanical or electrical load changes, can be amplified causing self-excitation, high mechanical stress of the drive train and even instability if no external damping controller is applied. A damping controller, implemented as illustrated in Figure 20, is acting similar to a power system stabilizer [27]. Its goal is to influence the generator electrical torque in such a way that it counteracts the speed oscillations and ensures a stable operation of the wind turbine. The idea of the proposed damping controller is to use the DC capacitor as a short-term energy storage, i.e. the speed oscillations are buffered and reflected in an oscillating defined DC-link voltage reference  $U_{DC}^{ref}$ . This oscillating reference, to which the DC-link voltage signal is controlled, generates a generator torque component, which counteracts and damps the speed oscillations.

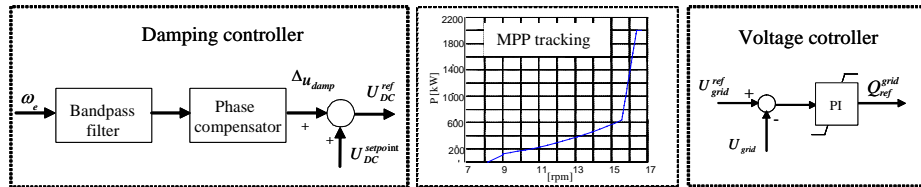


**Figure 20: Damping controller, maximum power point (MPP) characteristic and voltage controller.**

The generic control of generator-side converter is illustrated in Figure 21. It controls the DC-link voltage  $U_{DC}$  and the generator stator voltage  $U_s$  in the stator voltage oriented reference frame (SVRF). Hence, the DC voltage is controlled by the d-component of the stator current, while the stator AC stator voltage is controlled by the q-component of the stator current.

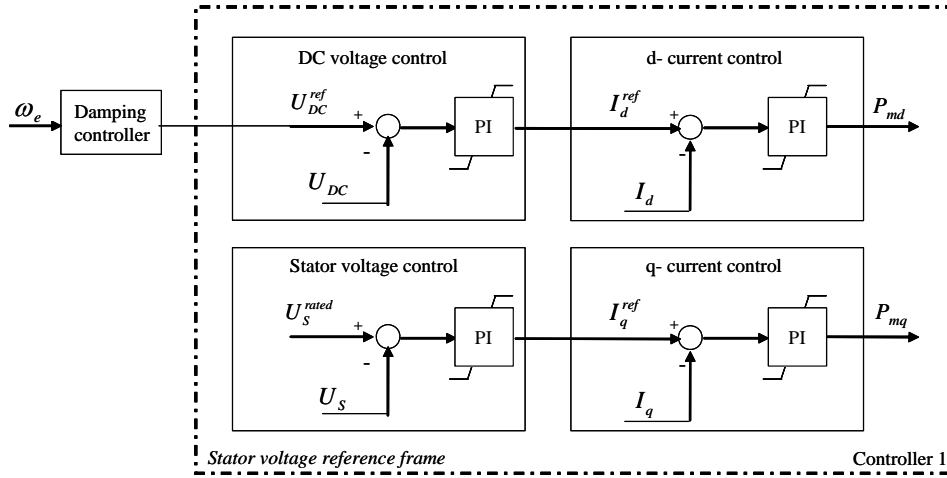


**Figure 21: Generator-side converter control (controller 1).**

The stator voltage  $U_s$  is controlled to its rated value  $U_s^{rated}$ . This strategy provides a robust control of the generator as it avoids the risk of overvoltage and saturation of the converter. The disadvantage is that it implies a variable reactive power demand from the generator, which must thus be delivered by a power converter with an increased rated power.

The DC-link voltage  $U_{DC}$  is controlled to its reference value  $U_{DC}^{ref}$ . This reference signal is provided by the damping controller and oscillates with the right frequency and phase angle, which generates a torque that dampens the speed oscillations. Notice that even though the idea is to keep the DC-link voltage constant and to ensure thus the power transport from the PMSG terminals to the power grid, small variations of the DC-link voltage are however allowed since the electrical damping of the system is necessary.

The generic control of the grid-side converter is illustrated in Figure 22. The grid-side converter controls independently the active power  $P_{grid}$  and the reactive power  $Q_{grid}$  in the grid voltage reference frame. Hence, the active power  $P_{grid}$  is controlled by the d-component of the converter current whereas the reactive power  $Q_{grid}$  is controlled by the q-component of the converter current.

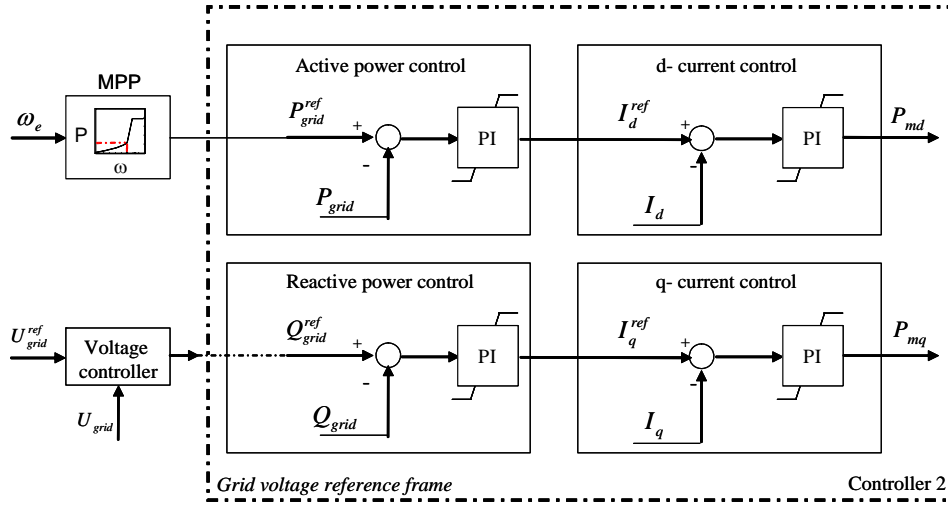


**Figure 22: Grid-side converter control (controller 2).**

When there is no particular active power demand from the system operator, the reference  $P_{grid}^{ref}$  for the active power is given by the maximum power point characteristic (MPP look-up) table, illustrated in Figure 20 as function of the optimal generator speed. The reference  $Q_{grid}^{ref}$  for the reactive power is typically set to zero, if no reactive power support is demanded. However, in the cases when the grid voltage is disturbed from its rated value and voltage grid support is demanded from the wind turbine, the reactive power reference  $Q_{grid}^{ref}$  can be provided by a voltage controller, as illustrated in Figure 22. Such a voltage controller is realized by a PI controller with antiwind-up and it controls the grid voltage to its rated value. The input of the controller is the error signal between the measured grid voltage and the rated grid voltage.

### 3.3.2 PMSG wind turbine control during grid fault operation

The overall control of the PMSG wind turbine during grid fault operation is illustrated in Figure 23 and described in details in [28].

Notice that the control uses an AC voltage oriented reference frame, i.e. d-axis to control the active current, while q-axis to control the reactive current. This means that in the generator-side converter's control, the DC-link voltage  $U_{DC}$  is controlled by the d-component of the stator current  $\hat{I}_d$ , while the AC stator voltage  $U_s$  is controlled by the

q-component of the stator current  $\hat{I}_q$ . In the grid-side converter's control, the active power  $P_{\text{grid}}$  is controlled by the d- component of the converter current  $\tilde{I}_d$  whereas the reactive power  $Q_{\text{grid}}$  is controlled by the q-component of the converter current  $\tilde{I}_q$ .

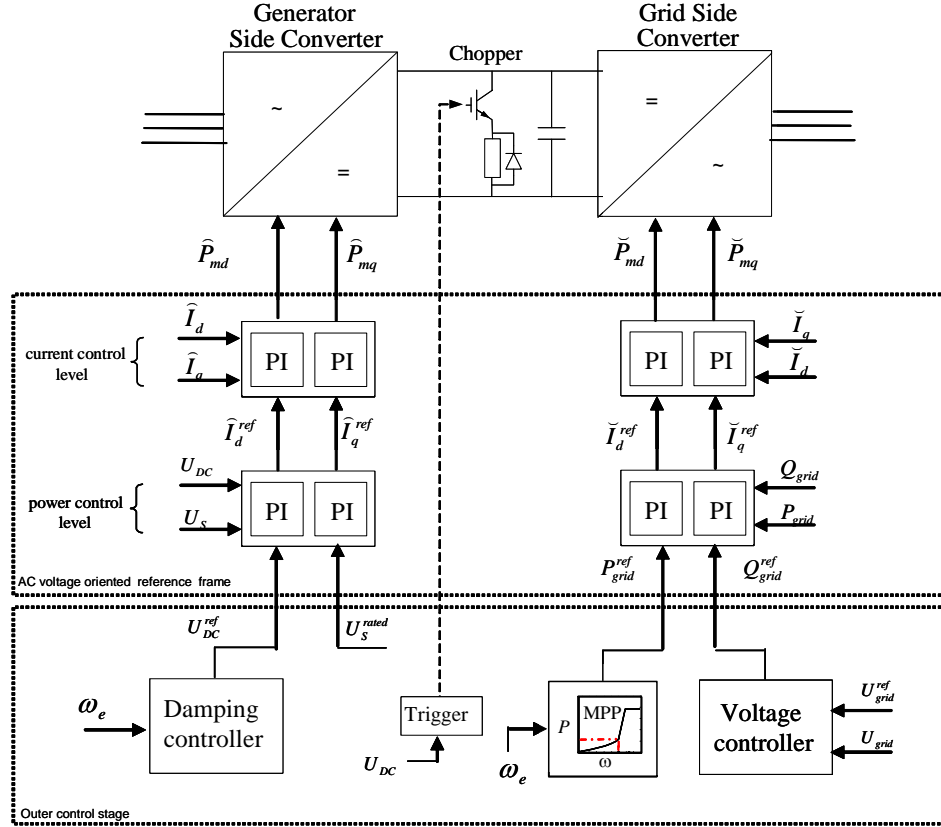


**Figure 23: Converter control strategy.**

Besides the reference signal for the stator voltage, all other reference signals for the power controller level are given by an outer control stage, as illustrated in Figure 23. The reference signal for the generator stator voltage  $U_s$  is chosen to be its rated value. The advantage of controlling the generator stator voltage  $U_s$  to its rated value is that the generator and the power converter always operate at the rated voltage, for which they are designed and optimized and over voltages in the converter can be avoided. The outer control stage contains a damping controller, a maximum power tracking characteristic and a voltage controller – as illustrated in Figure 23. Their design and performance have been presented in details in [28], and therefore only their main function is shortly addressed in the following.

If there is no particular active power reference specified by the power system operator, the reference  $P_{grid}^{ref}$  for the active power control is given by the maximum power point (MPP) characteristic, illustrated in Figure 23, as function of the optimal generator speed. This speed-power characteristic drives the turbine automatically in the operating point with the highest aerodynamic efficiency.

Notice that, since the PMSG generator is connected to the grid through a full-scale converter, only the active power of the generator is transferred to the grid. As the reactive power of generator cannot be exchanged through the DC-link in the converter system, the grid-side converter, whose electric frequency and voltage are fixed to the grid, can be set to control the reactive power/voltage on the grid. Notice that the reactive power production of the grid-side converter is thus independent by the reactive power set point of the generator, being limited only by the grid-side converter rating.

The reference  $Q_{grid}^{ref}$  for the reactive power is typically set to zero, if no reactive power support is demanded from the wind turbine. However, in the cases when the grid voltage is disturbed from its rated value and voltage grid support is demanded from the wind turbine, the reactive power reference  $Q_{grid}^{ref}$  can be assured by implementing a voltage controller, as illustrated in Figure 23. Such a voltage controller is realized by a PI controller with antiwind-up and it controls the grid voltage to its rated value. Depending on the difference between the measured grid voltage and the reference voltage, the voltage controller demands thus the grid-side converter controller to provide or to consume reactive power in order re-establish the grid voltage level.

In the control strategy presented here, sketched in Figure 23, the fault ride-through capability of PMSG wind turbine is directly integrated in the control design. In this control strategy, besides the stator voltage, the generator-side converter has to control the DC-link voltage. As the generator-side converter is not directly connected to the grid, and thus not affected during grid faults, it is able to fulfill its task to control the DC-link voltage undisturbed, also during faults. Meanwhile, as the grid-side converter is directly affected by grid faults, it can transfer less power to the grid than in normal operation conditions. As a consequence, the generator-side converter control reduces the generator power and thus the power flow to the DC-link, by decreasing the stator current, in order

to keep constant the DC-link voltage. Notice that the power imbalance, otherwise present in the DC-link during grid faults when the traditional control strategy is used, is transferred in this case to the generator. The power surplus is buffered in rotational energy of the large rotating masses. The power imbalance is thus reflected in the acceleration of the generator, which, in case when the generator speed increases above its rated value, is directly counteracted by the pitch controller, illustrated in Figure 18. Notice that, due to the sudden loss of electrical power, the drive train system acts like a torsion spring that gets untwisted. It starts therefore to oscillate. These torsional oscillations of the drive train are quickly damped by the designed damping controller

Notice that the simple reversal of the converter's functions in the new control strategy compared to the traditional one, makes it thus possible for the multi-pole PMSG wind turbine concept equipped with the new control strategy to ride-through during grid faults, without any additional measures, such as chopper or cross-coupling control between the generator-side converter and grid-side converter.

Nevertheless, a chopper can be however used to enhance even more the fault ride-through capability of a multi-pole PMSG wind turbine equipped with the new control strategy. The use of a chopper in this case can reduce the amplitude of the oscillations in the shaft torque and thus the mechanical stress of the drive train system during grid faults.

## **4. Generic large power system model**

In order to emphasize the fault ride-through and grid support capabilities of large wind farms, a realistic power transmission system model has to be used. Such a realistic model for the power transmission system is characterized by the voltage and the frequency that are not fixed to their respective rated values, but may be subject to fluctuations, when the transmission system is subjected to disturbances. The Danish Transmission System Operator Energinet.dk has developed a small test model for the power transmission system [29], especially for education and research purposes. This small test model embodies a generic simplified model of a power transmission grid, which is a fairly representative model to investigate the response of the transmission system with grid connected wind turbines to grid faults. It is implemented in the simulation tool



PowerFactory DIgSILENT and it produces a realistic output when the response of a whole wind farm has to be evaluated. The test model for the power transmission system in its original form, as described in [29], is used in the present investigations as basis for extension. The outline of the extended test model is presented in Figure 24. A detailed representation of data is provided in Table 1.

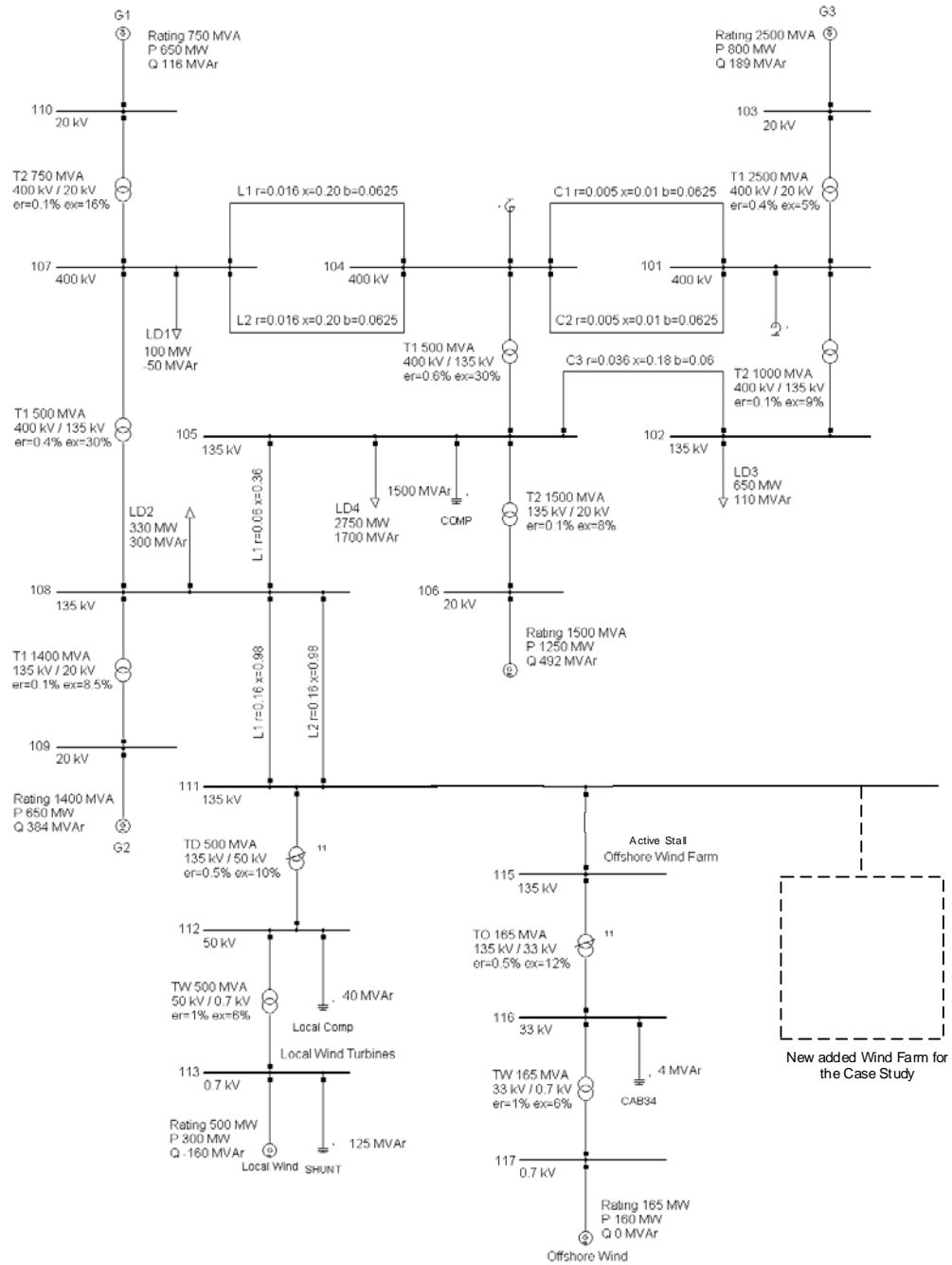


Figure 24: Generic power transmission system model –  
extended with a large wind farm.

The grid model contains busbars with voltages from 0.7kV to 400kV, four conventional power plants with their control, several consumption centres, a lumped

equivalent model for on-land local wind turbines and an aggregated model for a 165MW offshore active stall wind farm, connected through a sea cable to the transmission grid of 135kV. The conventional power plants are synchronous generators with primary voltage control. The model can be easily extended with frequency controllers, but as the attention in the present report is on voltage stability issues, it is assumed that the frequency stability in the system is assured only by large generator inertia.

**Table 1: Main data of synchronous generators and wind turbines.**

Parameters	G1	G2	G3	G4	Parameters	PMSG wind farm
Rated power [MVA]	750	1400	2500	1500	Rated power [MW]	165
Rated voltage [kV]	20	20	20	20	Rated voltage [kV]	3.3
Rated freq. [Hz]	50	50	50	50	Rated freq. [Hz]	50
Inertia [s]	5	5	5	5	Generator inertia [s]	0.91
Rotor Type	Round	Round	Round	Round	Rotor Type	Salient
$x_d$ [pu]	2.43	2.1	2	2.09	$x_d$ [pu]	1
$x_q$ [pu]	2.33	2	2	2.04	$x_q$ [pu]	0.9
$x_d'$ [pu]	0.307	0.365	0.3	0.254	$x_d'$ [pu]	0.99
$x_q'$ [pu]	0.6	0.7	0.7	0.39	$x_q'$ [pu]	0.99
$x_d''$ [pu]	0.2	0.2	0.2	0.2	$x_d''$ [pu]	0.99
$x_q''$ [pu]	0.2	0.2	0.2	0.2	$x_q''$ [pu]	0.99
$x_l$ [pu]	0.15	0.15	0.15	0.15	$x_l$ [pu]	0.05
$T_{d0}'$ [s]	7.5	7.4	6.6	6.6	$T_{d0}'$ [s]	0.00001
$T_{q0}'$ [s]	2.5	2.5	2.5	1.3	$T_{q0}'$ [s]	0.00001
$T_{d0}''$ [s]	0.029	0.041	0.04	0.038	$T_{d0}''$ [s]	0.0001
$T_{q0}''$ [s]	0.06	0.08	0.06	0.06	$T_{q0}''$ [s]	0.00009
Saturation $S_{1.0}$ [pu]	0.1	0.1	0.1	0.1	Saturation $S_{1.0}$ [pu]	—
Saturation $S_{1.2}$ [pu]	0.3	0.3	0.3	0.3	Saturation $S_{1.2}$ [pu]	—

Parameters	Local wind turbines	Active stall wind farm
Rated power [MW]	500	165
Rated voltage [kV]	0.7	0.7
Rated freq. [Hz]	50	50
Generator inertia [s]	0.5	0.5
Stator Resistance [pu]	0.006	0.006
Stator Reactance [pu]	0.08	0.08
Rotor resistance [pu]	0.018	0.018
Rotor Reactance [pu]	0.12	0.12
Mag. Reactance [pu]	4.4	4.4
Shaft Stiffness [pu/el.rad]	0.33	0.6
Rotor Inertia [s]	5	10

The on-land local wind turbines are fixed-speed, stall-controlled wind turbines equipped with no-load compensated induction generators. They are old land-based wind turbines without any ride-through control implemented and they are therefore disconnected from the system by the protection system in case of grid faults, to avoid over-speeding. The local wind turbines are aggregated in a lumped model representing all local wind turbines spread in the system with a total power capacity of 500MW. Aggregation methods reduce typically the complexity and simulation time without compromising the accuracy of the simulation results [15]. They can be especially used in power system studies concerning the impact of large wind farms on the power system. DIgSILENT Power Factory provides a direct built-in aggregation technique for the electrical system. The generator and the transformer can be directly modelled by a certain

number of parallel machines, while the other components, as e.g. the power converter or the mechanical power of the turbine rotor have to be up-scaled according to the wind farm power.

The 165MW offshore active stall wind farm, which is similar to the Danish offshore Nysted wind farm, is also modelled with a one-machine approach based on aggregation technique. The wind turbine lumped model contains models for the drive train, generator, transformer and the control, as described in detail in [29]. As required in [8], large wind farms connected to the transmission system have to be able to withstand grid faults without being disconnected in cases where the clearance of the fault does not isolate the wind farm. This is normally the case when the grid fault happens in the transmission system. In contrast to the local wind turbines, the active stall offshore wind farm, illustrated in Figure 24, is equipped with a fault ride-through capability control, namely in case of a severe voltage drop, the active power production is reduced to avoid uncontrolled overspeeding (i.e. the mechanical power of the rotor is directly ramped down to 20% of the rated mechanical power). The reduction of the active power production implies that the reactive power absorption is reduced too. Such power reduction control has a positive effect, contributing to a better stabilisation of the wind farm. It is a kind of passive reactive power control as it does not participate actively in the voltage control of the system.

The power system test model, described in [29], is extended in this present study by an aggregated offshore wind farm consisting exclusively of 80 equal 2MW PMSG wind turbines – see Figure 24. This wind farm is connected to the transmission system at a 135 kV busbar through an offshore line just like in the connection case of the offshore active stall wind farm. This additional wind farm is also modelled by one equivalent lumped wind turbine with re-scaled power capacity according to the entire wind farm power.

According to [27], the interaction between the grid and units, i.e. wind farms, connected to it, depends on the strength of the AC system relative to the capacity of the connected units. The point of common coupling (PCC) busbar of the connected wind farms in the power system model illustrated in Figure 24, is a “weak” connection point and therefore the study of the support capabilities of the large wind farms connected to such a grid is of high relevance.

## 5. Fault ride-through capability

The main goal of fault-ride through requirement is to avoid significant loss of wind turbine production in the event of grid faults. Fault ride-through solutions for different wind turbine concepts are investigated in the wind turbine industry and presented in the literature. The behavior of wind turbines during grid faults has initiated an important research activity.

This chapter addresses the fault ride-through capability of different wind turbine concepts with their possibilities and limitations.

### 5.1. ASIG wind turbines' response to grid faults

In this work, the ASIG wind turbine control strategy during grid faults is implemented based on [17]. The idea is that during the fault, the ASIG wind turbine normal controller, illustrated in Figure 8 is switched off and replaced by a control strategy to reduce directly the mechanical power of the rotor to a predefined level. The ordering of power reduction is given for example when the monitoring of the grid voltage indicates a fault occurrence. When the grid fault is cleared, the wind turbine continues running at reduced power for still few seconds, after which it starts to ramp up the mechanical power of the rotor and re-establish the control for ASIG wind turbine normal operation conditions.

Figure 25 shows how an active stall wind turbine equipped with fault ride-through capability behaves during a grid fault. A 3 phase short circuit closest to the wind turbine, i.e. on 10kV busbar, that lasts for 100ms is simulated. It illustrates the behavior of an active stall wind turbine equipped with reduced power control during grid faults. As expected, the generator voltage drops right after the grid fault and recovers to its initial value when the fault is cleared after 100ms. During grid fault, the turbine accelerates as the aerodynamic torque is no longer balanced by the electromagnetic torque of the generator. The rotor speed of the ASIG wind turbine reflects the power system frequency behavior during the fault. When the fault occurs, the speed is initially increased due to the acceleration of the conventional generators and after that it drops below nominal value.

Notice that, as soon as the fault is detected, the normal operation control strategy is switched off and replaced by the open loop fault operation controller, which has to reduce the power production to a predefined level. The reduction of the wind turbine mechanical power is applied to assess the fault ride-through capability of the active stall wind farms. As illustrated in Figure 25, the pitch angle ramps down to a fault operation pitch setpoint. The change in the pitch angle is limited by the pitch rate limiter existing in the servo mechanism. As soon as the fault is cleared and the voltage is recovered to the required range, the wind turbine continues still running at reduced power for still few seconds, before it ramps up the mechanical power of the rotor.

The pitch system ramps then up the pitch angle to its normal operation conditions value.

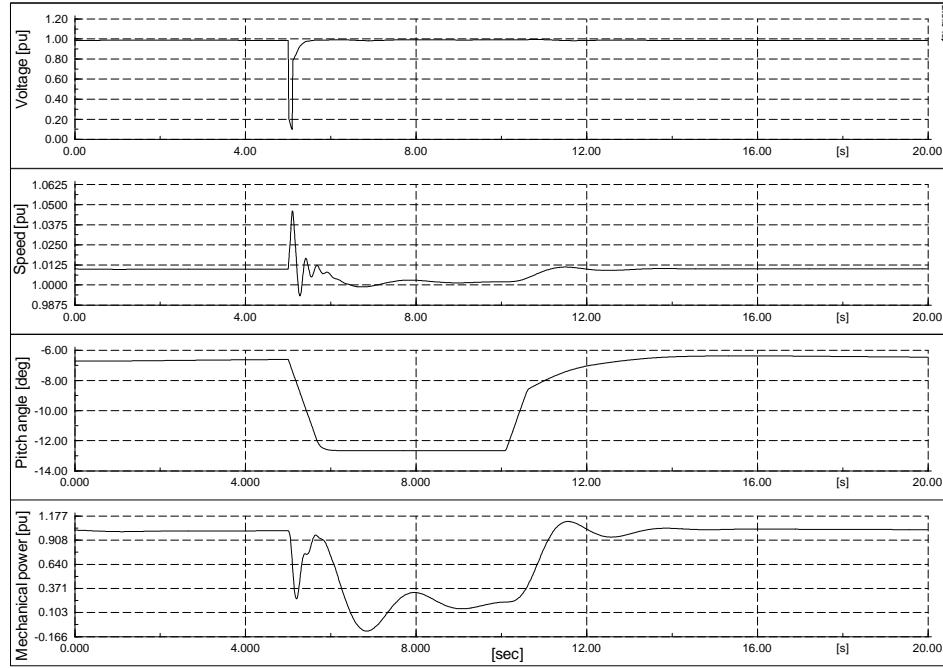


**Figure 25: ASIG wind turbines' response to grid faults.**

During the grid fault the ASIG wind turbine absorbs reactive power during the low voltage conditions. After the initial peak in the reactive power, shown in Figure 26, the wind farm absorbs reactive power, threatening the voltage stability of the system. The reactive power in Figure 26 is measured in the PCC, and includes the power delivered to the grid by the capacitor banks installed at the wind farm bus to reduce the negative effect on reactive power-voltage control of the system during severe faults.

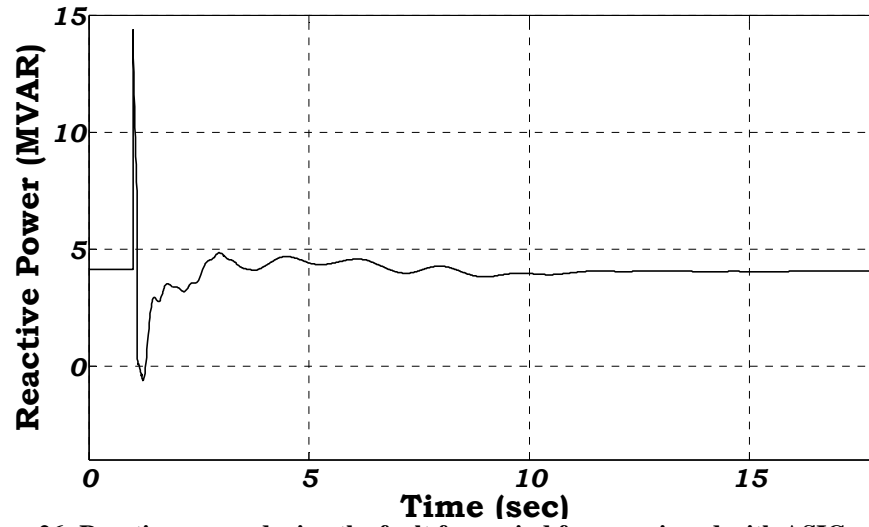


Figure 26: Reactive power during the fault for a wind farm equipped with ASIG wind turbines.

## 5.2. DFIG wind turbines' response to grid faults

The specific converter arrangement in the DFIG configuration requires advanced protection system, because of the high inrush stator and rotor currents during grid faults.

A simple protection method of the DFIG under grid faults is to short circuit the rotor through a device called crowbar. The crowbar protection is an external rotor impedance, coupled via the slip rings to the generator rotor instead of the converter. The value of the crowbar resistance is dependent on the generator data and therefore in case of another generator, a new value of the external rotor resistance has to be chosen [21]. The function of the crowbar is to limit the rotor current. When the crowbar is triggered, the rotor side converter is disabled and bypassed, and therefore the independent controllability of active and reactive power gets unfortunately lost. Generator magnetization is in this case done over the stator, instead of being done over the rotor circuit by the rotor side converter. Since the grid side converter is not directly connected to the generator windings, where the high transient currents occur, this converter is not blocked for protection.

In normal operation of a DFIG wind turbine, the active power reference for the rotor side converter is given by the maximum power tracking (MPT) point characteristic as function of the optimal generator speed [19]. In the case of a grid fault, this power reference is defined as the output of a damping controller [6]. The damping controller is

attenuating the oscillations in the drive train produced by the grid fault. It ensures the fault ride-through capability of the wind turbine, i.e. avoids an eventual wind turbine grid disconnection due to undamped oscillations in the generator speed. When a fault is detected, the definition of the power reference is thus switched between the normal operation definition (i.e., MPT) and the fault operation definition (damping controller). Notice that the pitch control system is not able to damp the torsional oscillations, because of several delay mechanisms in the pitch [6]. The pitch control damps the slow frequency variations in the generator speed, while the damping controller is able to damp the fast oscillations in the generator speed.

Figure 27 illustrates the effect of the damping controller in case of a 100 ms three phase grid fault at the high voltage terminal of the 3-windings transformer of a 2MW DFIG wind turbine. It is assumed that the wind turbine works at its rated power at the fault instant. As the fault operation is small compared to the wind speed fluctuations, the wind speed can be assumed constant in the grid fault simulations. The generator speed, the mechanical torque, the pitch angle and the aerodynamic power of the wind turbine are illustrated for the situations with and without damping controller, respectively.



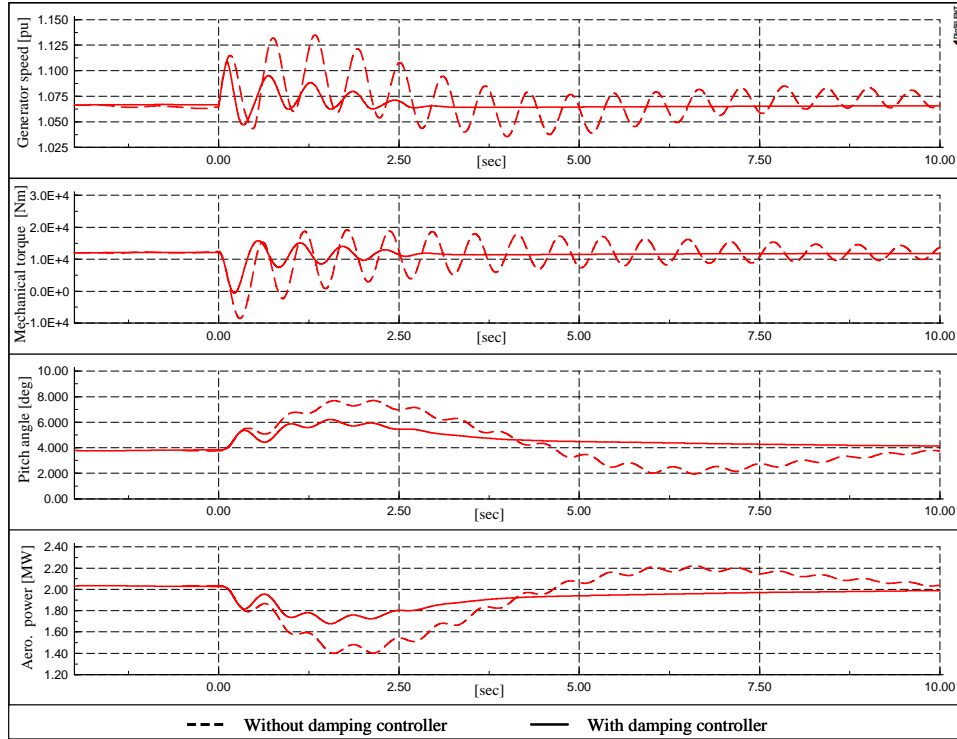


**Figure 27: Improved DFIG performance during grid fault when a damping controller is used.**

Note that without the damping controller, the torsional oscillations excited by the grid fault are only slightly damped still 10 seconds after the grid fault incident. It is clearly visible that the oscillations are quickly damped over few seconds when the damping controller is used. Furthermore the amplitude of the mechanical torque is much smaller when using the damping controller. Moreover, in contrast to the case when no damping controller is used, the mechanical torque crosses only once through zero when the damping controller is used, and therefore the mechanical stress of the drive train is substantially reduced in this case.

As expected, during the fault, the turbine starts pitching in order to counteract the acceleration of the generator. Note that the pitching activity is lower and more effective during the fault, when the damping controller is used. This implies both a more constant aerodynamic power and a lower stress of the pitch system. The use of the damping controller has thus a positive effect both on the pitch angle and on the aerodynamic power. Hence the presence of the damping controller is very important for minimizing the grid fault effect both on the mechanical and on the electrical side of the turbine.

The protection system together with the damping controller enhances thus the DFIG fault ride-through capability.

The dynamic interaction between variable speed DFIG wind turbines with the power transmission system illustrated in Figure 24 during and immediately after grid faults is illustrated and explained in the following. The power system in Figure 24 is used in the following investigation in the simplified layout illustrated in Figure 28.

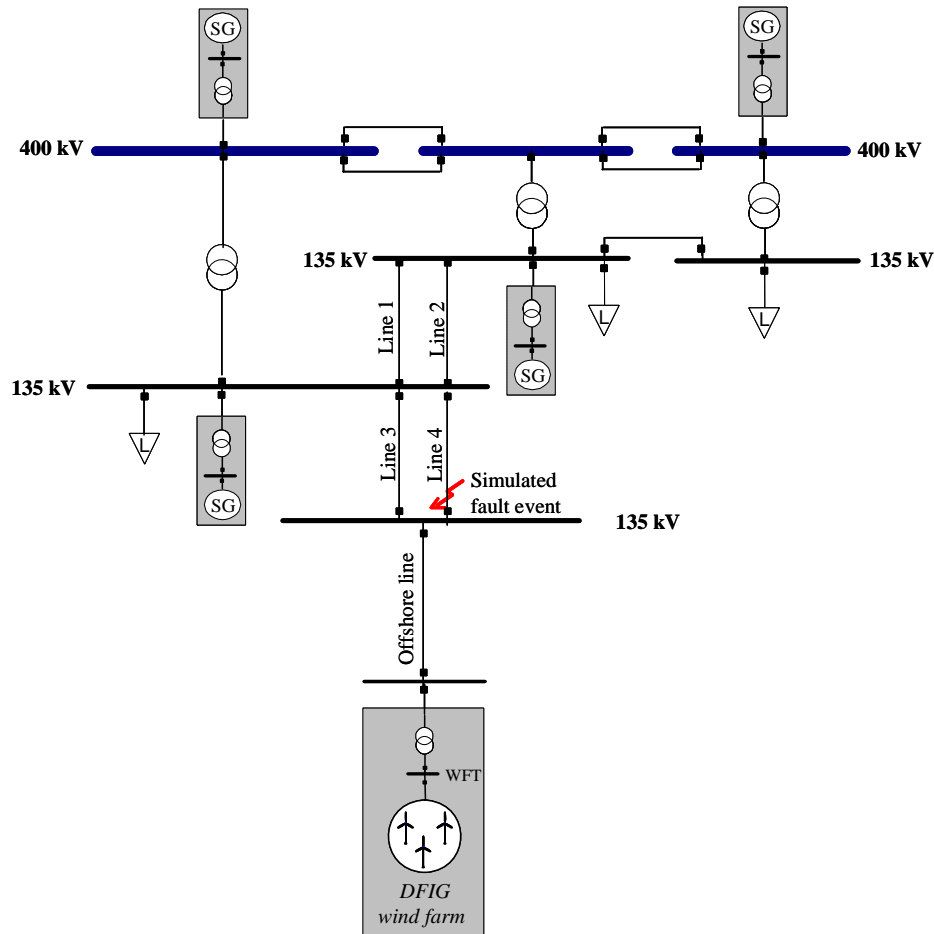


**Figure 28: Layout of the studied power system only with DFIG wind farm.**

The new included wind farm, consisting of 80 equal 2MW DFIG wind turbines, is connected to the transmission system at a 135 kV busbar through an offshore line, as illustrated in Figure 28. The offshore wind farm is modelled with a one machine approach based on the aggregation technique described in [15]. The one DFIG turbine

with re-scaled power capacity and equipped with a crowbar protection system is modelled and controlled as described in the report.

A severe three phase short circuit grid fault is considered to happen in the transmission grid at the end of Line 4 close to the wind farms, as illustrated in Figure 28. The grid fault lasts for 100 ms and gets cleared by permanent isolation (tripping the relays) of the faulty line (Line 4 in Figure 28). Note that, by tripping Line 4, the power system becomes weaker (higher impedance) and some components (e.g. Line 3) are fully loaded. During the grid fault, it is assumed that the DFIG wind farm operates at its rated capacity.

The evaluation of the dynamic interaction between the DFIG wind turbines and the power system model, during and shortly after the short circuit fault at the end of Line 4, is discussed by means of the simulation results presented in the following, in Figure 29 and Figure 30. A grid fault affects both the mechanical and electrical components of the wind turbine. The mechanical time constants are much larger than the electrical, and therefore the mechanical and the electrical effects can not be illustrate in the same time frame. As the mechanical aspects of a DFIG wind turbine during a grid fault has been illustrated in Figure 27, the focus in the following is on the electrical signals of the DFIG wind turbine, in a time frame about 500 ms.

### ***Behavior immediately after the fault***

In the fault instant, the voltage at the DFIG generator terminal drops and it leads to a corresponding decrease of the stator and rotor flux in the generator. This result in a reduction in the electromagnetic torque and active power – see Figure 29. As the stator flux decreases, the magnetization that has been stored in the magnetic fields has to be released. The generator starts thus its demagnetization over the stator, which is illustrated in Figure 29 by the reactive power peak in the moment of the fault. As the electromagnetic torque of the generator drops according to the voltage drop too, the torsion spring in the drive train gets untwisted and therefore the mechanical torque drops too. However the drop of the mechanical torque is slower than of the electromagnetic torque and therefore the generator starts to accelerate. The dynamic relation between the electrical torque, mechanical torque and the generator speed is reflected in Figure 29.

Notice that the over-speeding of the generator during the fault is counteracted by the pitch control system.

In the fault moment, as the stator voltage decreases significantly, high current transients appear in the stator and rotor windings – see Figure 30. Note that the rotor current resembles the stator current. In order to compensate for the increasing rotor current, the rotor side converter increases the rotor voltage reference, which implies a “rush” of power from the rotor terminals through the converter. On the other side, as the grid voltage has dropped immediately after the fault, the grid side converter is not able to transfer the whole power from the rotor through the converter further to the grid. The grid side converter’s control of the dc-voltage reaches thus quickly its limitation. As a result, the additional energy goes into charging the dc-bus capacitor and the dc-voltage rises rapidly – see Figure 30.

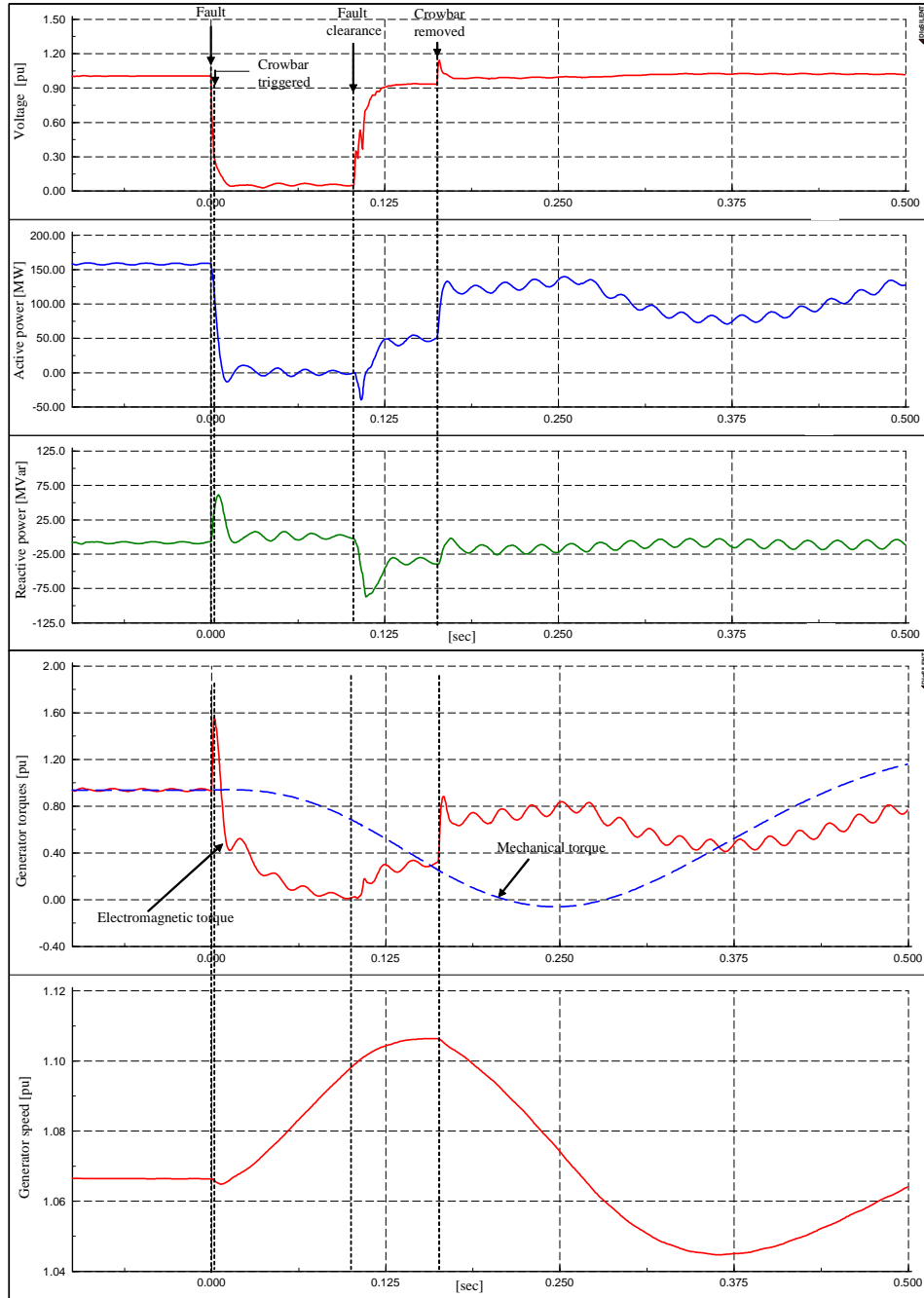


**Figure 29: Generator's terminal (WFT) voltage, active power, reactive power, electrical torque, mechanical torque and speed.**

Exceeding the limit of the rotor current or of the dc-voltage activates the protection system. This short circuits the generator rotor by triggering the crowbar. The rotor side converter is blocked and therefore its control of the rotor currents is disabled. In the

moment the crowbar is triggered, the dc-bus capacitor starts discharging; the grid side converter begins to control the dc-link voltage back to its reference. Note that, as long as the crowbar is triggered, the generator behaves as a conventional squirrel cage induction generator (SCIG), namely the converter rotor voltage output is zero – as illustrated in Figure 30.

### ***Behavior after fault clearance***

Immediately after the fault is cleared, the stator voltage is restored, the electromagnetic torque and active power start to increase – see Figure 29. As the grid voltage and the flux increases, the demagnetised stator and rotor oppose this change in flux leading thus to an increase in the rotor and stator currents – see Figure 30. Note that when the fault is cleared, the voltage does not recover completely immediately. Just after fault clearance, it reaches a voltage level lower than its nominal value, while it reaches completely its nominal voltage level after the removing of the crowbar. The reason for that is that just after fault clearance the generator continues to behave as squirrel cage induction generator and therefore it starts to absorb reactive power for its magnetization – see Figure 29. The rotor side converter is disabled until the crowbar is removed, and therefore it is not able to provide the reactive power necessary for the magnetization of the generator. The generator absorbs thus reactive power from the grid and this action delays the recovering process of the grid voltage.

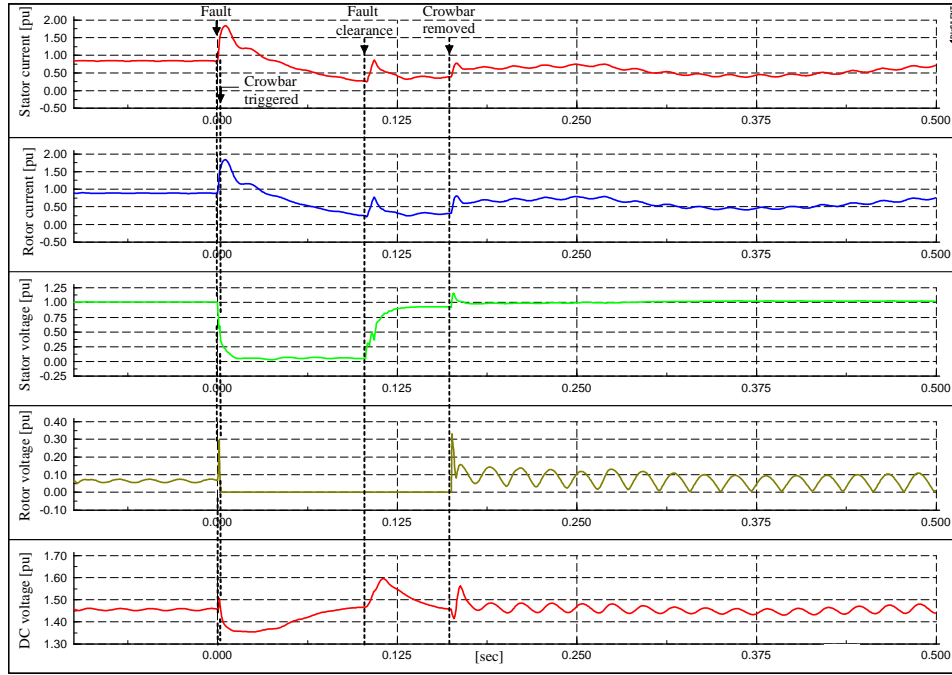


**Figure 30: Generator currents and voltages.**

When the grid voltage recovers over a certain value, the crowbar is removed. From this moment, the voltage recovers completely, the generator currents and voltages start to converge to their pre-fault values and the rotor side converter starts actively to control the active and reactive power.

The detailed simulations illustrated in Figure 29 and Figure 30 provide a quick overview and a better understanding of the functionality of the DFIG wind turbine control and protection during grid fault.

### 3.4 Multi-pole PMSG wind turbines' response to grid faults

Figure 31 and Figure 32 illustrates firstly how the full-scale converter multi-pole PMSG wind turbine equipped with the new control strategy is able to ride-through grid faults without any additional measure and secondly how the use of a chopper can enhance the turbine's fault-ride through capability even further.

A 100 ms three phase short circuit is considered to occur at the high voltage terminal of the 2-windings transformer of the PMSG wind turbine. The PMSG wind turbine is connected to a grid, which is modeled as a Thevenin equivalent. It is assumed in the simulation that the voltage controller is disabled and that the wind turbine operates at its rated power first without any chopper attached. As illustrated in Figure 31, the voltage

drop occurs at the grid fault instant. Due to this drop, the grid-side converter can only transfer a reduced amount of active power  $P_{\text{grid}}$  to the grid during the fault. However it is able to continue to control the reactive power to its initial reference value. Notice in Figure 31, which during the grid fault the generator power and the power inserted in the grid have a similar characteristic. On the other hand, the grid power is kept constant after the fault has been cleared, while the generator power presents an oscillated behavior, as expected, which is however quickly damped, i.e. in less than 4 sec, by the damping controller. Meanwhile, when no chopper is used, the generator-side converter has to reduce the generator power, in order to be able to keep the DC-voltage constant. This action leads to a power imbalance between the reduced generator power and the unchanged aerodynamic turbine power. As result, the generator starts to accelerate and the drive train gets untwisted and starts to oscillate, as illustrated in Figure 31.

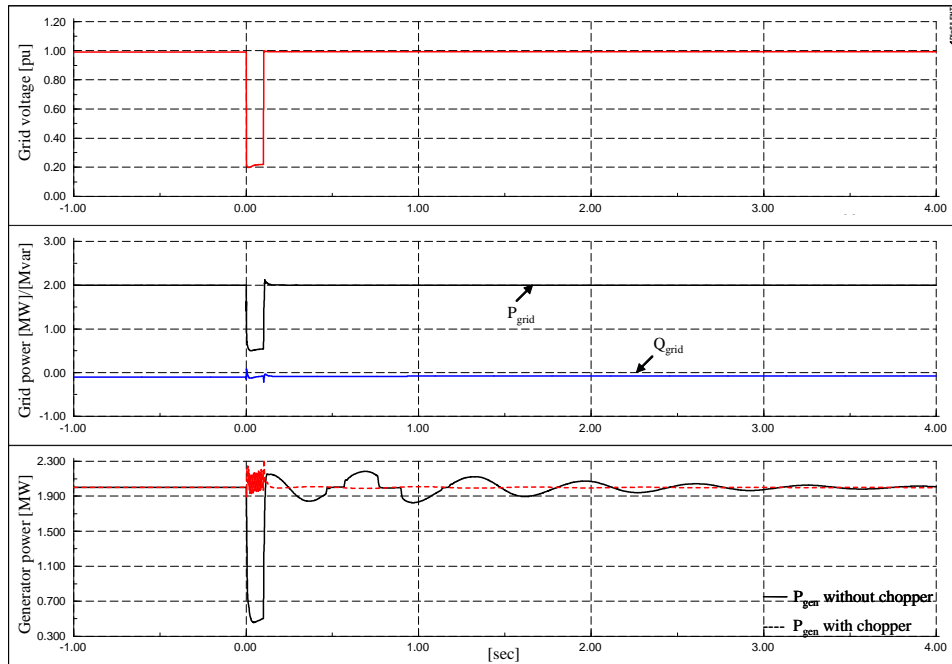


**Figure 31: Fault ride-through capability of full-scale converter multi-pole PMSG wind turbine equipped with the alternative control strategy.**

The acceleration of the turbine is less than 2%, due to the large inertia of the turbine's rotor. The torsional oscillations in the drive train are visible both in the



mechanical torque, generator speed and the DC-link voltage. Notice that they are quickly damped by the damping controller.

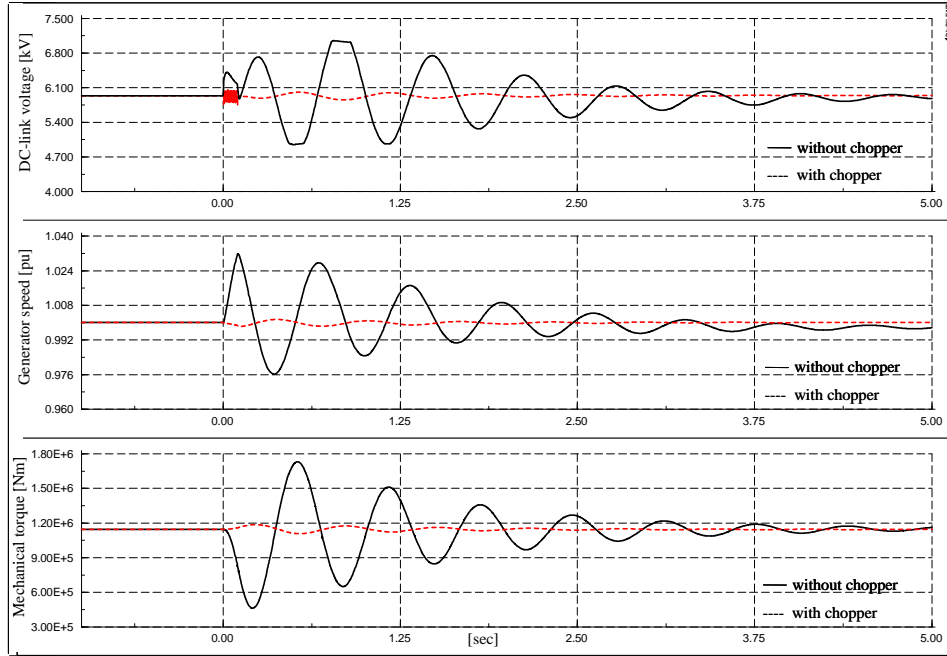


**Figure 32: Grid fault impact on the DC-link voltage, generator speed and on the shaft torque with and without chopper.**

The simulations in Figure 31 and Figure 32 illustrate clearly that the wind turbine equipped with the new control strategy, is able to ride-through grid faults without any additional measures. In addition to this, the figures show also that the use of a chopper during a grid fault, when the new control strategy is applied, can enhance the turbine's fault ride-through capability even further. Notice that, when a chopper is used, the surplus power in the DC-link is burned in the chopper and, as shown in Figure 31, it is therefore not necessary to reduce the generator power. Figure 32 shows how the generator acceleration and drive train oscillations are significantly reduced when a chopper is used. It is also clearly illustrated that the chopper reduces effectively the grid fault impact on the wind turbine mechanical stress (i.e. smaller oscillations in the shaft torque) and enhances even further the PMSG wind turbine's fault ride-through capability.

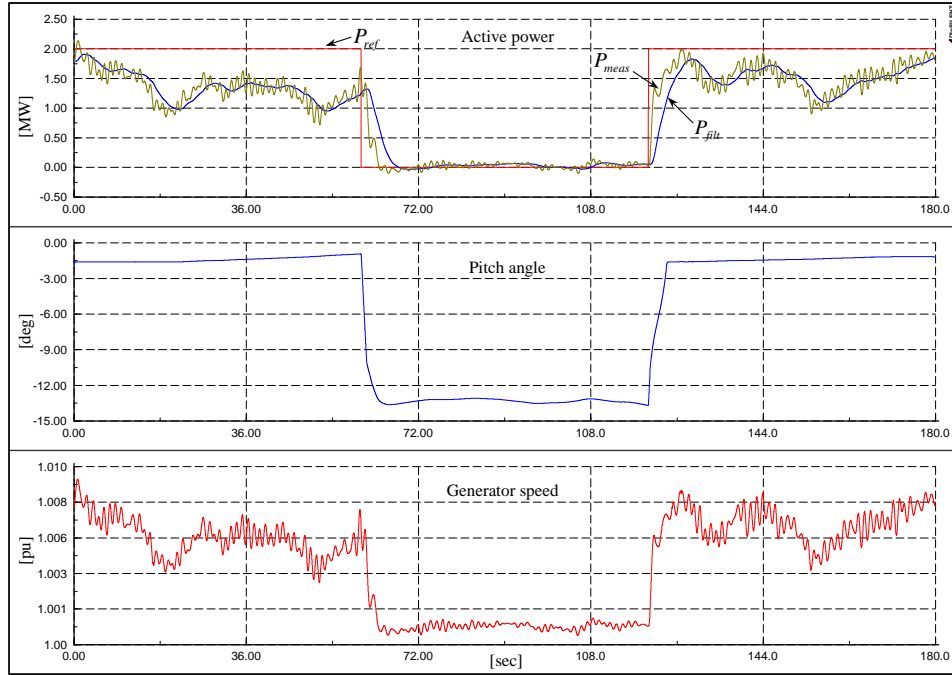
## **6. Power grid support**

The increased wind power penetration in the electrical power system implies that the status of wind turbines is changing from being simple energy sources to power plant status with grid support characteristics, i.e. power grid support.

Different scenarios are simulated in the following to illustrate the grid support capability of different wind turbine concepts like active stall wind turbine, doubly-fed induction generator wind turbine and multi-pole permanent magnet full scale converter wind turbine. The controller's performance is assessed and discussed by means of a set of simulations of a 2 MW active stall wind turbine.

### **6.1 ASIG wind turbines' power grid support**

Figure 33 and Figure 34 present simulation results of the proposed power control strategy of the active stall wind turbine, shown in Figure 8 and Figure 10, respectively. The active stall wind turbine is simulated at an average wind speed of 11 m/s and a turbulence intensity of 20%. This operational point for the wind turbine corresponds to a transition operational regime for the wind turbine, between power optimization and power limitation regime, where the 3p fluctuation (three times the rotational frequency) is strong.



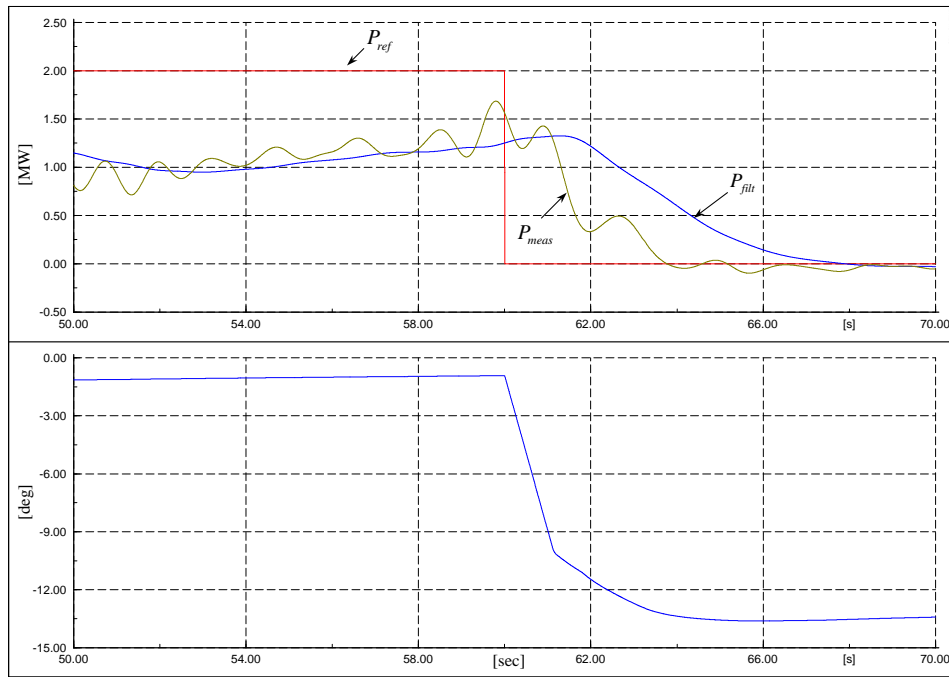
**Figure 33: Power reference response of an active stall controlled wind turbine.**

Figure 33 shows the reference power  $P_{ref}$ , the measured power  $P_{meas}$  at the MSP and the filtered measured power  $P_{filt}$  used in the controller, together with the pitch angle and generator speed, respectively. As expected for an active stall wind turbine, the 3p fluctuation is present in the measured electrical power  $P_{meas}$ . In order to illustrate the performance of the active stall wind turbine controller, the following sequence is assumed. The first 60 sec, the power reference is set to the rated power (i.e. 2 MW). The power reference is then stepped down to 0 MW and after 120 sec it is stepped back again to 2 MW.

In the first and last 60 sec of the simulation, by setting the power reference equal to the rated power for a wind speed less than the rated wind, the wind turbine has to produce maximum possible power. In this case the pitch angle is set by the upper limit of the controller given by the “optimal pitch” look-up table – see Figure 8. The wind turbine is then ordered to work in the power limitation mode when the power reference is set to 0 MW. In this control mode, the turbine has to produce less than it is capable of and therefore the power controller starts to actively drive the measured power to the power reference. The controller has been tuned so that the pitch angle changes smoothly from one steady state operational point to another without any overshoot. A reduction of the

power production implies a more negative pitch angle and a smaller generator speed (slip). The demand of producing 0 MW is achieved while the wind turbine operates close to the border between generator and motor modes.

Figure 34 gives a more detailed view on the power and the pitch angle in the moment when the power reference is stepped down to 0 MW. The new power reference is reached in 4-5 seconds. The change in the pitch angle is limited by the pitch rate limiter  $\pm 8 \text{ deg/s}$ , which exists in the actuator.



**Figure 34: Detailed view of the power reference responses illustrated in Figure 33.**

Figure 35 illustrates the simulation results for the reactive power control, sketched in Figure 10. The simulation case is the same as shown in Figure 33. The reactive power at the MSP is controlled to zero by switching on or off a certain number of capacitors. In the present simulation a capacitor bank consisting of 12 steps with 0.1 MVar is used. A clock with 20 ms sampling period ensures a necessary fast switch of the capacitors. With this fast sampling period, as seen in Figure 35, the reactive power is changed immediately by capacitor switchings as soon as the reactive power exceeds the hysteresis interval  $\pm 150 \text{ kVar}$ . Figure 35 also shows the number of capacitors switched during the simulation. Notice that, as expected, a step down in the active power reference implies a

reduction of the reactive power demand and, as a result, the number of connected capacitors is decreased.

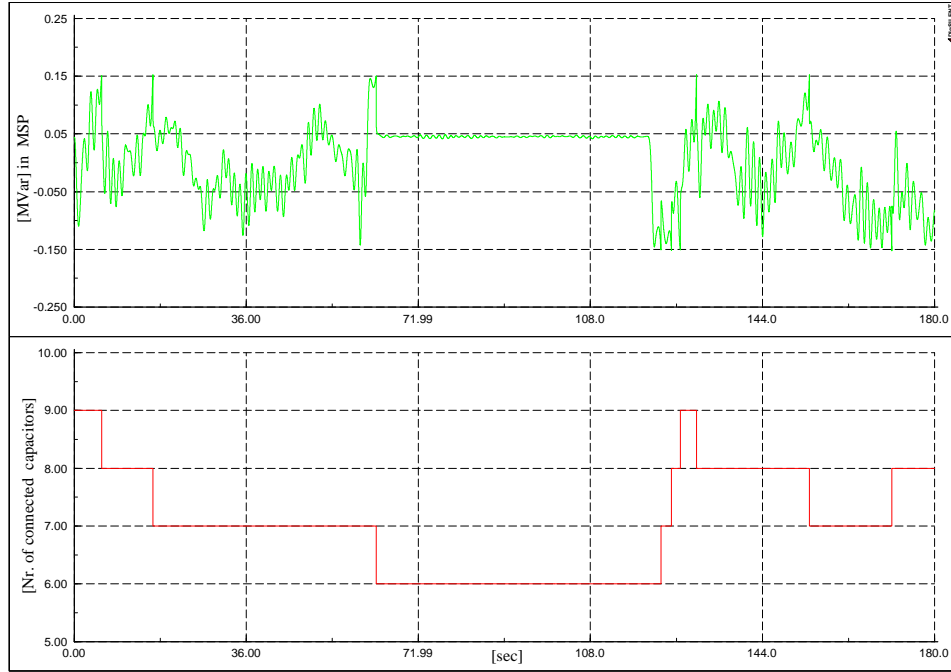


**Figure 35: Reactive power control for the active stall controlled wind turbine.**

The focus in the next simulations is on the wind farm controller performance in the PCC of the active stall wind farm. Therefore the simulation results only at the wind farm level are presented. Figure 36 illustrates the performance of the wind farm power controller, when the active power demands from the grid operators is stepped down and up to different setpoints. The reactive power reference for the whole wind farm is kept to zero. The wind turbines in the wind farm are driven by different turbulent winds with 9 m/s mean speed value and 10% turbulence intensity. Figure 36 shows the estimated available power, the power demand, the power reference and the measured power in the PCC of the wind farm. In order to test the performance it is assumed that the power demand from the operator is first stepped down from 6 to 2, 1 and 0 MW and then stepped up in reverse sequence.

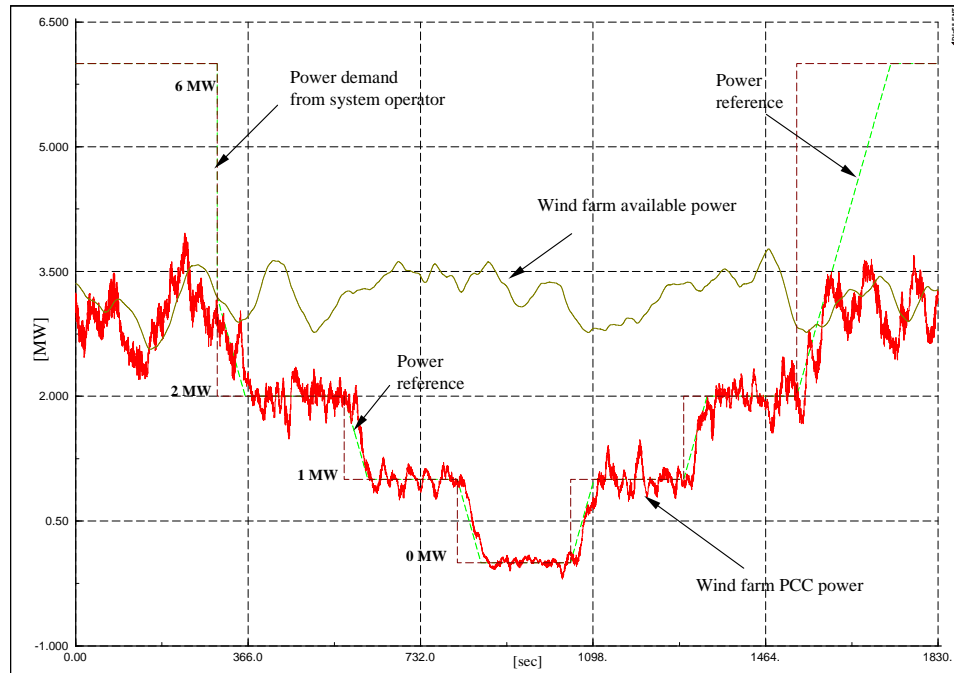


**Figure 36: Wind farm response in balance control with stochastic wind speed of 9m/s and turbulence intensity of 10%.**

The first and last 300 sec, the wind farm performs a normal operation and it has to produce maximum power. Notice that in this operation mode, the power reference is set to the rated power of the whole wind farm. The wind farm controller is designed in such a way that in normal operation, it allows the wind farm to produce more than the wind farm estimated available power, if this is possible. The production is thus not restricted to the estimated available power and therefore unnecessary pitch activity at each wind turbine is avoided. Note in Figure 36, that in the first and last 300 sec, the wind farm has the possibility to produce more than the estimated available power. At the wind turbine level this is reflected by a low pitch activity, the pitch angle being kept nearly constant to the optimal pitch value.

The simulation results show a good performance of the control system. The adjustment upwards and downwards of the wind farm production is performed with a power ramp rate limiter of about  $\pm 1.2 \text{ MW} / \text{min}$ . In power limitation mode the wind farm production follows properly the wind farm elaborated power reference, taking the power ramp rate limiter into account. Notice that the power fluctuations decrease at lower power references. The demand of producing 0 MW is achieved properly by the wind farm. At

the wind turbine level this is reflected by a slight oscillation in the machine's speed between generator and motor modes.

Figure 37 illustrates the performance of the wind farm controller, when the reactive power demand from the grid operator is stepped up and down to different set points. There are two graphs: the first shows the whole sequence while the second provides a detailed view on the reactive power response at a step moment in the reactive power demand. The wind turbines are again driven by different turbulent winds with 9 m/s mean speed and 10% turbulence intensity. It is assumed that the wind farm is ordered to have maximum active power production. In order to test the performance of the reactive power wind farm controller, it is assumed that the reactive power demands from the operator are stepped up from 0 to 1, 2 and 3 respectively and then stepped down vice versa. Notice that the adjustments upwards and downwards of the wind farm reactive power production are performed very quickly as long as the size of capacitor bank permits that. The new reactive power reference is reached in less than 0.5 seconds. This quick performance is attractive from a grid support point of view. At a wind speed 9 m/s, each wind turbine generator produces around 1.1 MW and consumes about 0.5Mvar. This means that the whole wind farm consumes about 1.5 MVar. As each wind turbine presents a capacitor bank with 12 steps, each of 0.1 MVar, it means that for a wind speed about 9 m/s, the wind farm has a reactive power reserve of about 2 MVar. This is clearly illustrated in Figure 37, when the 3 MVar reactive power demand cannot be reached.

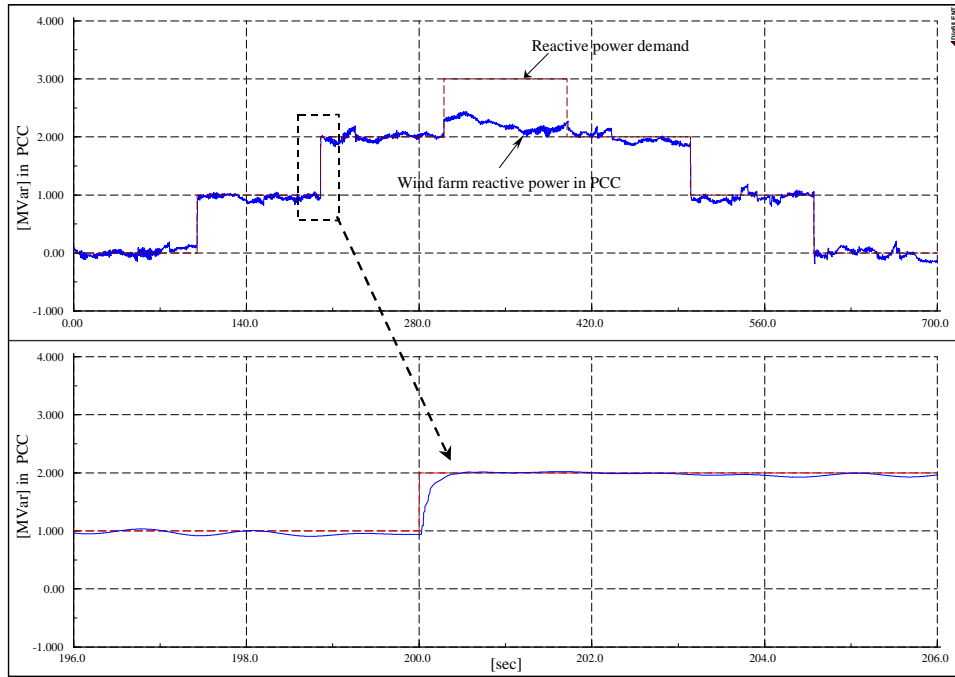


**Figure 37: Reactive power response for the wind farm**

## 6.2 DFIG wind turbines' power grid support

Simulation results for normal operating conditions are given in Figure 38 and verify the designed control strategy. Figure 38 illustrates the wind speed, the pitch angle, the generator speed as well as the active and reactive power production in case of turbulent wind with a mean wind speed of 12 m/s and a turbulence intensity of 10 %. The signals of pitch angle, speed and active power reflect the stochastic character of the wind and are tracking the slow variations of the wind speed. For wind speeds below rated wind (approx 12 m/s) the power and speed are adapted to the point of maximum aerodynamic efficiency. For wind speeds above rated wind the pitch mechanism is active and the power is limited to its rated value. However, independent of the fluctuations of the wind, active and reactive power can be controlled to imposed reference values. Inspired by [10] the control system is set to follow a specified sequence: In the time period between 30 s and 60 s a reactive power demand of 0.5 MVar is required from the turbine. Notice, that the active power production is not influenced by the step in reactive power. Between 80 s and 170 s the active power reference is stepped down first to 1 MW and then to 0 MW



and is then stepped up back again. The turbine is however only capable to follow this reference if the wind speed is sufficiently high. Notice, that a reduced reference power implies higher changes in pitch angle and generator speed. Finally between 200 s and 230 s the wind turbine is demanded to absorb 0.5 MVar reactive power from the grid, which is also very well accomplished. Figure 6 points out, that the designed control strategy of the variable speed wind turbine model with DFIG is able to control active and reactive power independently to specific imposed reference values, exactly as a conventional power plant does.

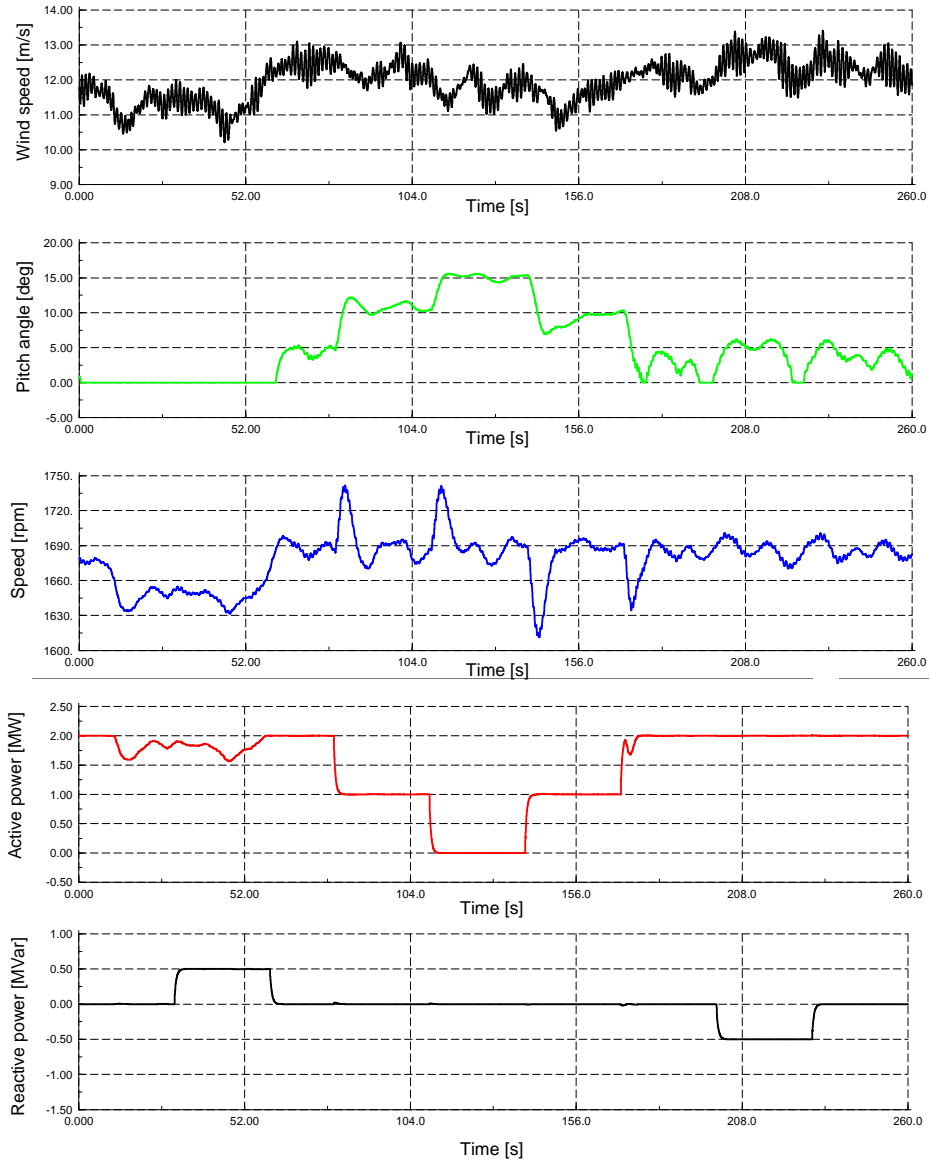


**Figure 38: Control of active and reactive power of DFIG.**

Figure 39 shows the simulation of a normal operation of a 6MW variable speed DFIG wind farm, when it is ordered to performed balance control, delta control, the power gradient limiter and the reactive power control. The wind turbines in the wind farm are driven by different turbulent winds, with 9 m/s mean speed value and 10% turbulence intensity. Figure 39 illustrates both the available and the actual active power and the reactive power measured in the PCC of the wind farm, when the system operators

require different control actions. In order to test the wind farm controller, the following active power control functions sequence is proposed:

The first 100 sec the wind farm has to produce maximum power. Notice that the actual power follows the available power as long as the ramp limiter permits that.

The time period between 100 sec and 420 sec a delta control is imposed. The wind farm has to operate with a 0.5 MW constant reserve capacity.

The time period between 200 sec and 320 sec a balance control is imposed. The wind farm is ordered to regulate downwards to 2 MW. Notice that in this period, both the delta and the balance control are active at the same time. The adjustment upwards and downwards of the wind farm production is performed with a ramp limitation about  $\pm 1.2$  MW/min.

The time period between 420 sec and 700 sec maximum power production is again ordered.

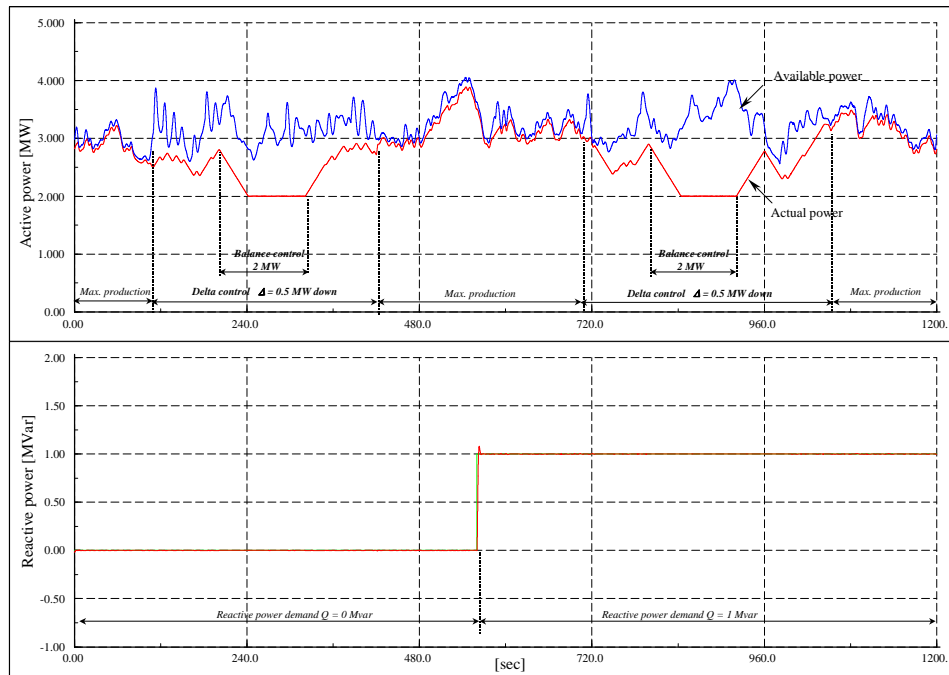


**Figure 39: Wind farm control level: maximum production, delta control, balance control, ramp limiter. At time 560 sec the reactive power reference is changed from 0 Mvar to 1 Mvar.**

The reactive power reference for the whole wind farm  $Q_{ref}^{WF}$  is set to zero the first 560 sec. A step in the wind farm reactive power demand to 1 MVar is then applied at 560 sec

and the previous active power control functions sequence (1-4) is repeated. Notice that the generated active power is not altered by the step in the reactive power demand, its variations being only due to the turbulent wind. The simulation results show a good performance of the control system. The specified references both for the active and reactive power are achieved properly.

### **6.3 Multi-pole PMSG wind turbines' power grid support**

Figure 40 presents simulation results where the multi-pole PMSG wind turbine assists the power system. The capability to control independently the active and reactive power production to the grid is also illustrated. The wind turbine is simulated at an average wind speed of 11m/s and a turbulence intensity of 10%. This operation point corresponds to a transition operational regime for the wind turbine, between power operation and power limitation regimes. In order to illustrate the performance of the wind turbine's control system, the following sequence is assumed. During the first 80 s, the wind turbine has to produce maximum active power. In this case the pitch angle is set to zero as the wind turbine works in the power optimization regime, while the speed tracks the slow variations in the wind speed. The power reflects the optimal power according to the generator speed and the MPP look-up table. The time period between 30 and 60s a reactive power demand of 1MVar is required from the wind turbine. Notice that the generated active power is not altered by the step in the reactive power demand, its variations being only due to the turbulent wind. In the time period between 80 and 170s, the active power reference is first stepped down to 1MW, then after 30s down to 0MW and then it is stepped back again to 1MW after 30s and then finally back to maximum power demand at the time 170s. In this control mode the turbine has to produce less than it is capable of and therefore the grid-side converter controller starts to actively drive the measured power to the imposed power reference. A reduction of the power production implies as expected an increased pitch angle and generator speed. The time period between 200 and 230s, the wind turbine is demanded to absorb 1MVar from the grid - a request which is also very well accomplished.

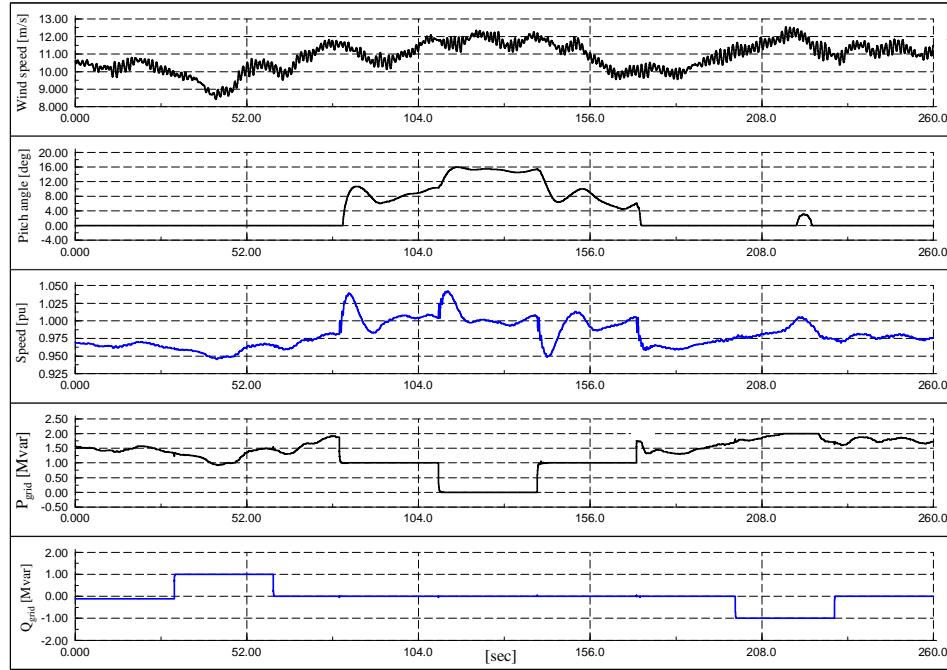


**Figure 40: Power grid support. Simulation sequence: during 0 - 80s maximum active power demand; during 30 – 60s reactive power demand of 1MVar; at time 80s active power demand of 1MW; at time 110 s active power demand of 0MW; at time 140s active power demand of 1MW; during 170 – 260s maximum active power demand; during 200-230s reactive power demand of -1MVar.**

The simulation results indicate good performance of the presented control system. The specified references both for the active and reactive power are achieved properly. This illustrates that if it is required, the multi-pole PMSG wind turbine can operate as a conventional power plant, i.e. it can produce or absorb reactive power and it can adjust actively its active power production according to system operator demands.

## 7. Voltage grid support

During grid faults the system voltage drops in vicinity to the location of the fault. In order to support the voltage level and voltage re-establishment by the wind turbines, voltage control and reactive power supply are required by transmission system operators. The ability to deliver reactive power to the grid is strongly dependent on the wind turbine

technology. Grid codes require not only compensation of the wind turbine's own reactive power demand but also additional reactive power supply in dependency of the voltage dip.

This chapter addresses the voltage grid support capability of different wind turbine concepts with their possibilities and limitations.

## **7.1. ASIG wind turbines' voltage grid support**

In order to illustrate the voltage grid support of an active stall wind farm equipped with a capacitor bank, the network layout illustrated in Figure 41 is used. The wind farm consists of three fixed speed active stall wind turbines, each of 2 MW rated power. The wind farm is connected to a 10 kV busbar in a 50/10 kV station. A two- winding transformer is installed in the station. Each of the three wind turbines WT1, WT2, WT3 are connected to its own 10 kV terminal. Both the connection of the wind farm to the station and the station itself are modelled by the actual physical components (transformers, line, busbar).

The layout of the active stall wind turbine is shown in Figure 6. Each wind turbine is connected to a 10 kV busbar. The induction generator, softstarter, the capacitor bank for reactive power compensation and the step-up transformer are all placed in the nacelle. The control of capacitor bank is based on measured reactive power at the Main Switch Point MSP.

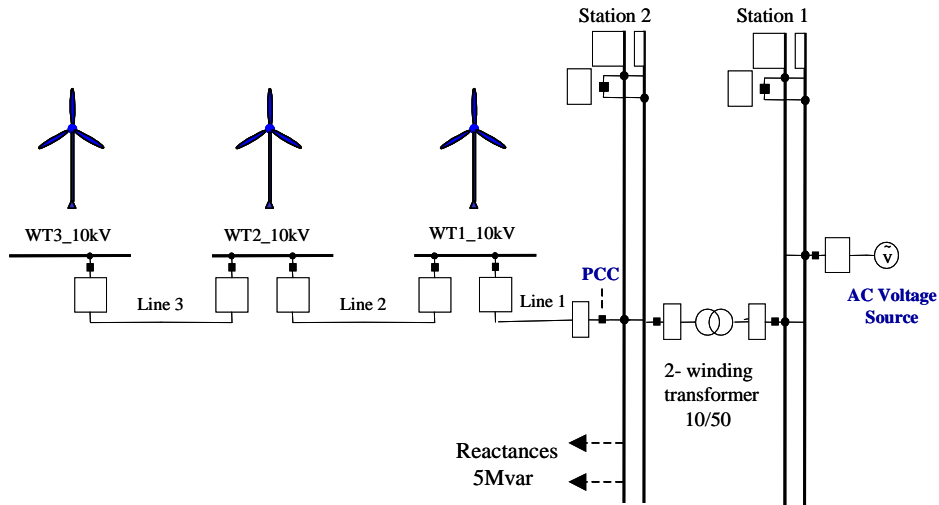


**Figure 41: Layout of active stall wind farm with AC connection.**

Figure 42 illustrates the case when the wind farm is driven by constant wind speeds of 9 m/s. In order to show the voltage control it is assumed that a 5MVar reactance is connected to the 10 kV busbar – see Figure 41 at the time moment of 10 sec and a second reactance on the same size is further connected in the same place at the time moment of 20 sec. Figure 42 shows the voltage in PCC and the deadband of the voltage control, the reactive power reference corrections  $\Delta Q_{volt}$  and the reactive power in the PCC of the whole wind farm. Notice that the connection of the first reactance implies a modification in the voltage in PCC, which is still inside voltage deadband. However, the subsequent connection of the second reactance to the 10 kV busbar leads to a further reduction of the voltage in PCC. This time the voltage is outside the deadband. In this point in time the reactive power reference is corrected. The wind farm is thus ordered produce more reactive power in order to compensate for the decrease of the voltage at PCC. The new reactive power reference is then reached quickly by the controller.

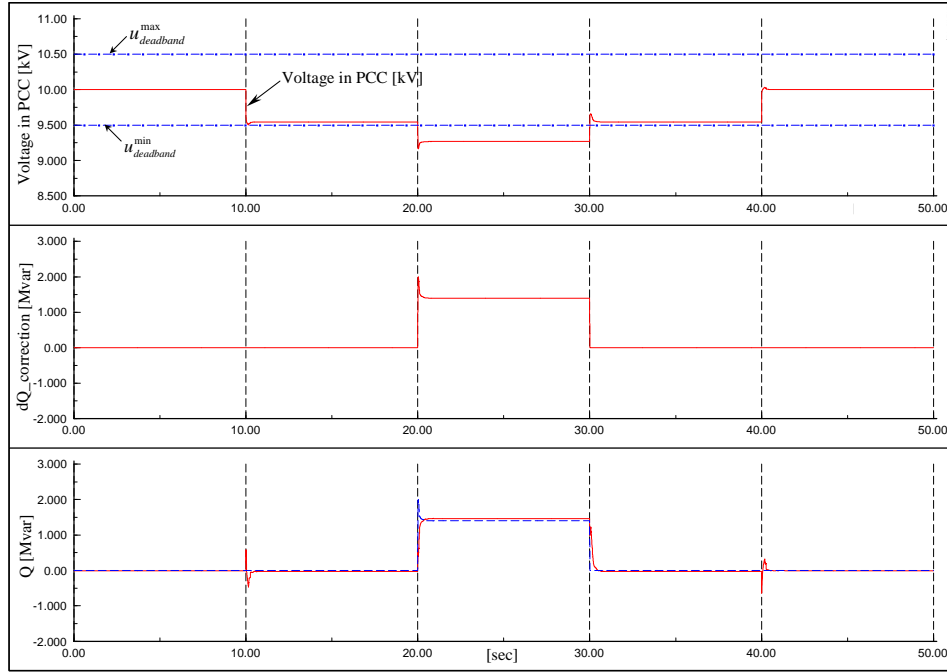


**Figure 42: Voltage control when two reactances of 5Mvar are connected and disconnected sequentially.**

## 7.2. DFIG wind turbines' voltage grid support

In order to illustrate the DFIG voltage grid support capability, an extended model of the test model for the power transmission system in described in [29] and shown in Figure 24, is used in the following. As illustrated in Figure 43, the test model is extended by adding a new offshore wind farm, made up exclusively of DFIG wind turbines. The new wind farm consists of 80 equal 2MW DFIG wind turbines. It is connected to the transmission system at a 135 kV busbar through an offshore line just like in the connection case of the offshore active stall wind farm. The new wind farm is modelled based on the aggregation technique, namely by one equivalent lumped wind turbine with re-scaled power capacity. It is also equipped with the co-ordinated voltage control, described in the report. A worst case for the voltage stability is considered. It is thus assumed that, during the grid fault, the DFIG wind farm operates at its rated capacity. The wind farm is modeled with a one-machine approach based on the aggregation technique.



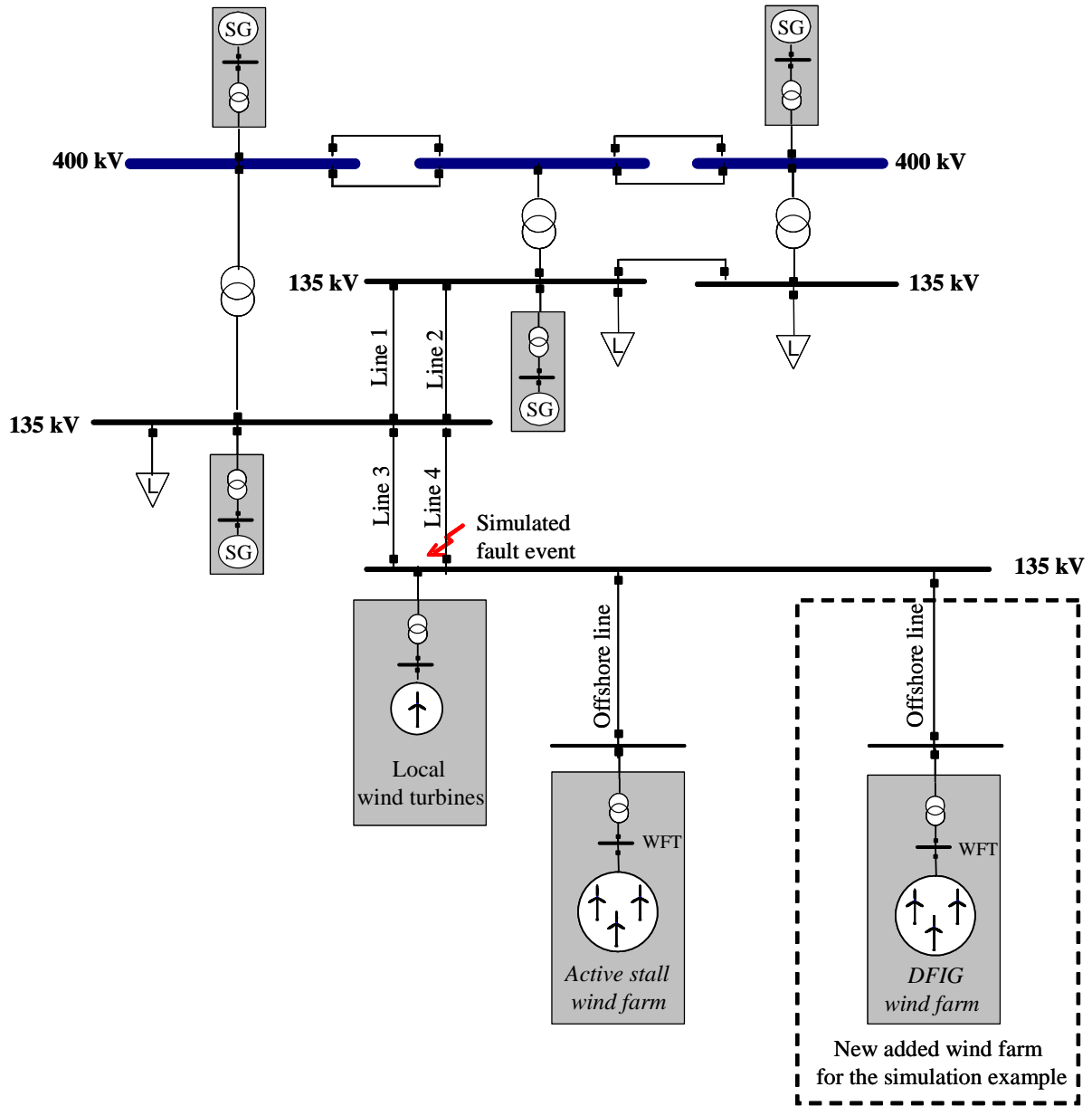


**Figure 43: Layout of the power system for the study of voltage support of DFIG wind farms.**

Figure 44 illustrates the voltage, the active and the reactive power of the DFIG wind farm in the wind farm terminal (WFT), for the situations with and without DFIG voltage grid support respectively.

As expected, the influence of voltage grid support is visible both during grid fault, when the GSC operates as STATCOM and supplies reactive power, and after the disconnection of the crowbar, namely when the RSC controls the voltage on the grid. When no DFIG voltage grid support is enabled, the grid voltage oscillates as expected.

After a while, it stabilizes to a higher voltage level. This aspect can be explained both by the reactive power surplus existent in the system as result of the on-land wind turbines' disconnection and by the fact that, as result of the fault clearance (tripping Line 4), the transport of the active power from the wind farms to the grid is done through a higher resistance transmission line.

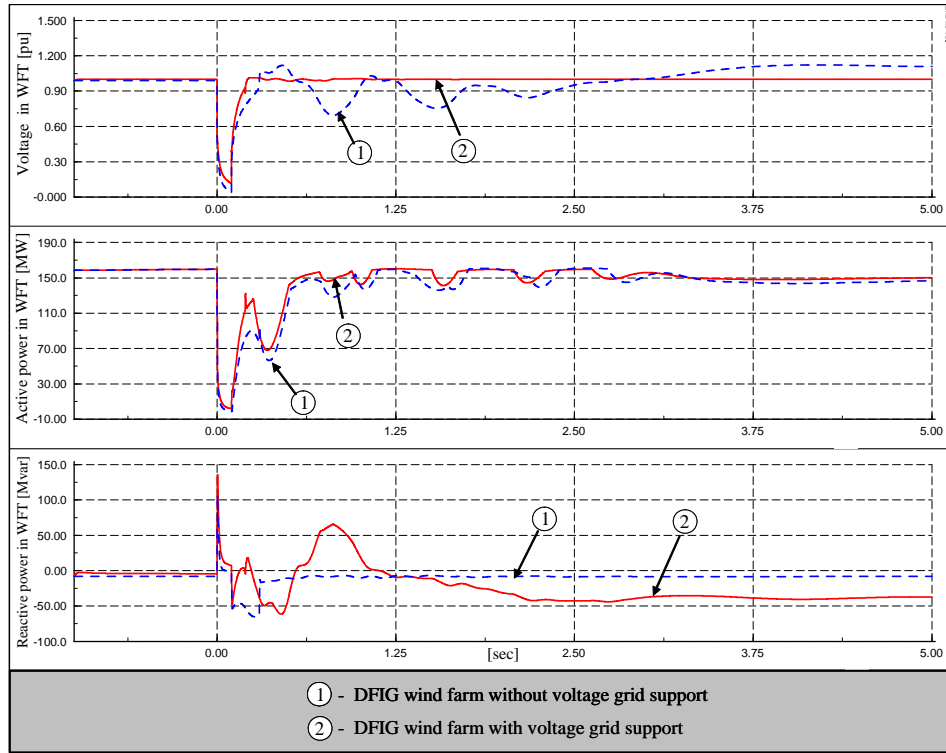


**Figure 44: DFIG wind farm terminal with and without voltage control when the power reduction of the active stall wind farm is disabled.**

Figure 44 shows that the existing reactive power surplus in the system is absorbed by the DFIG, when the voltage grid support control is enabled. Note that the DFIG voltage control re-establishes the grid voltage to 1p.u. very quickly without any fluctuations. No significant effect of the voltage control appears on the active power production. However, there it is a slight improvement in active power when voltage control is used. The small “drops” in the power, visible in both cases just after the fault is cleared, are generated by the damping controller used to damp torsional oscillations in the generator speed of the DFIG after the grid fault. Similarly to Figure 27 these oscillations are damped over few seconds. The initial level of the active power is reached after few more seconds.

In Figure 44 the attention is focused on the performance of the DFIG wind farm during a grid fault when it is or not equipped with voltage control. One question in mind is now how the DFIG wind farm voltage control influences the performance of a nearby active stall wind farm during a grid fault, placed as it is illustrated in Figure 24. The next two figures, i.e. Figure 45 and Figure 46, contain therefore only information concerning the active stall wind farm during the grid fault, namely the active and the reactive power in the wind farm terminal, the generator speed and the mechanical power of the active stall wind turbines, respectively.

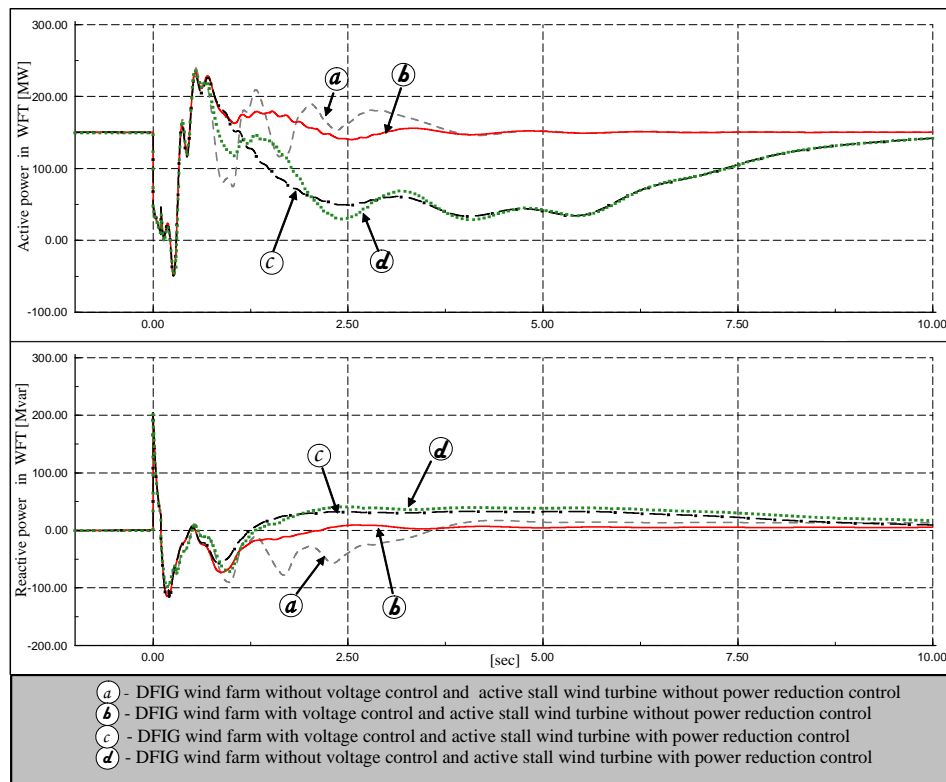


**Figure 45: The active and the reactive power of the active stall wind farm in different 4 situations.**

Both Figure 45 and Figure 46 illustrate the simulation results from the following four different control sceneries:

- DFIG wind farm without voltage control and active stall wind farm without power reduction control.
- DFIG wind farm with voltage control and active stall wind farm without power reduction control.

- DFIG wind farm with voltage control and active stall wind farm with power reduction control.
- DFIG wind farm without voltage control and active stall wind farm with power reduction control.

The following remarks are concluded:

- The voltage control of the DFIG wind farm (case b and c) has a damping effect on the mentioned signals of the active stall wind farm, no matter whether this has power reduction control or not.
- The active power, the generator speed and the mechanical power are almost identical during the grid fault, no matter which case is simulated. The fact that the mechanical power is unchanged in this period means that the drive train system is equally stressed in all 4 cases.
- The worst case for the active stall wind farm is clearly the case a, when the DFIG wind farm has no voltage control and the active stall wind farm has no power reduction control.
- The best case for the active stall wind farm is clearly the case b, when DFIG wind farm is equipped with voltage control, and the power reduction control of the active stall wind farm is not enabled. Note that the wind farm is not subjected to torsional oscillations and there is no loss in the active power production. The influence of the DFIG voltage control on the active stall wind farm is thus even better when the latter does not have any special control implemented to ride-through a grid fault.

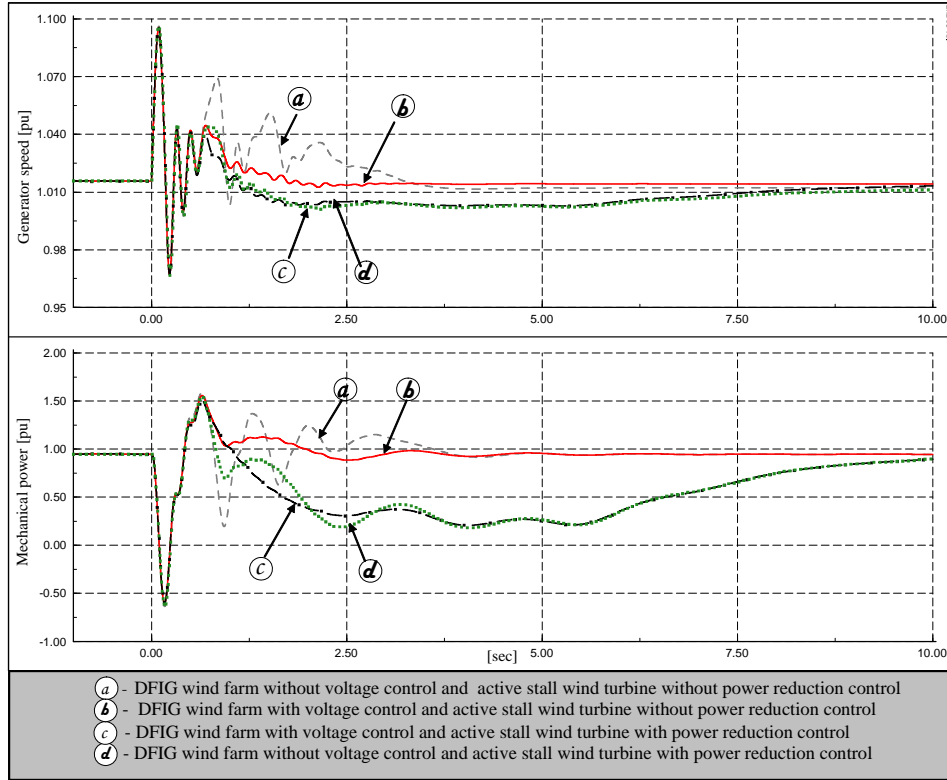


**Figure 46: Generator speed and mechanical power of the active stall wind farm in different situations.**

The overall conclusion from the last two figures is that the DFIG wind farm equipped with voltage control can help a nearby active stall wind farm through a grid fault, without any need to implement additional ride-through control strategy in the active stall wind farm.

### 7.3. Multi-pole PMSG wind turbines' voltage grid support

To assess the performance of the voltage controller, presented in Figure 22, a simulation is performed with two reactive power sinks (one of 1MVar and the other of 1.5MVar) connected at the MV terminal of the PMSG wind turbine and disconnected after 1 sec, successively.

The grid voltage and the reactive power supplied to the grid by the grid-side converter are illustrated in Figure 47 for the situations with and without voltage controller, respectively. It is assumed that the 2MW PMSG wind turbine operates now at

its rated capacity (i.e. at wind speeds higher than 12m/s), as this is worst for voltage stability.

Notice that the connection of each reactance implies as expected a drop in the grid voltage  $U_{\text{grid}}$ . The voltage drop is about 22% when the 1MVar reactance is connected and about 30% when the second 1.5MVar reactance is connected later. When no voltage control is enabled (case 1 in Figure 47), no reactive power support is delivered to the grid by the grid-side converter. The voltage drop is not compensated by reactive power and the voltage recovers to its nominal value only when the reactance is disconnected.

On the other hand, when the voltage controller is used (case 2), the grid-side converter supports the grid by supplying reactive power – as illustrated in Figure 47. The voltage controller notices the deviation in voltage and commands more reactive power. The increased reactive power supplied by the grid-side converter re-establishes the grid voltage to 1pu in less than 100ms when the first 1MVar reactance is connected. Notice that the supplied reactive power is higher than the value of the connected reactance 1MVar. The reason is that the converter also has to compensate for the reactive power absorbed by the transformer placed between the grid-side converter and the PCC. The 2MW PMSG wind turbine connected to the grid through the 2.5MVar converter has a reactive power reserve about 1.5MVar when it operates at its rated capacity, as it is the present case of 12m/s wind speed. Notice that the voltage is not completely re-established when 1.5MVar is connected even though the voltage controller is enabled. The reason for this is that the reactive power reserve of 1.5MVar of the converter is reached in this case.

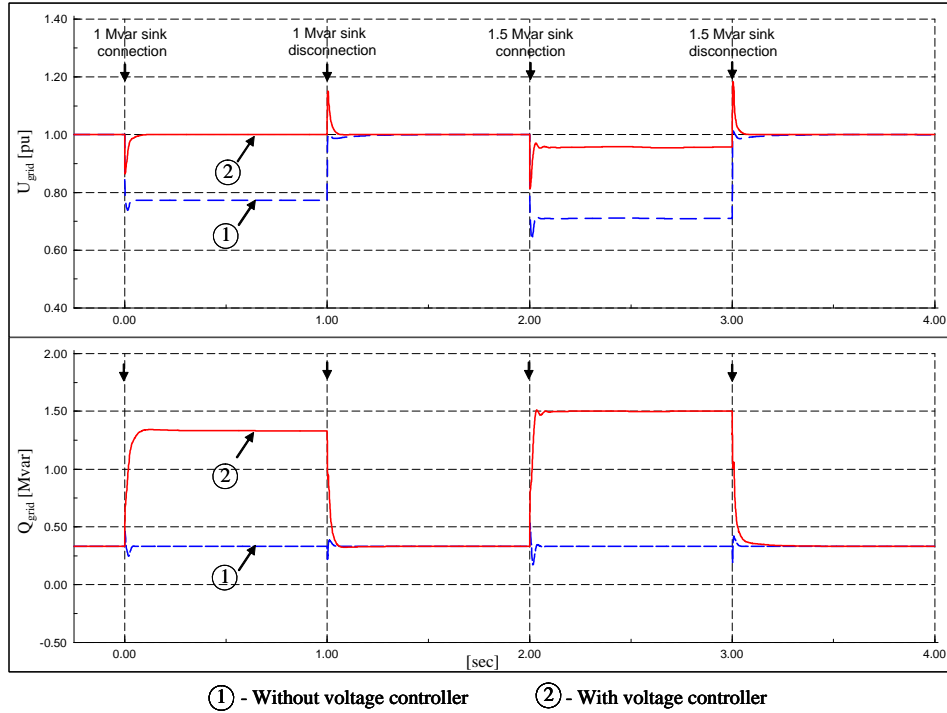


**Figure 47: PMSG voltage controller performance ((1) – without voltage control (2) with voltage control) -when a reactive power sink of 1Mvar and 1.5Mvar respectively, is connected and disconnected.**

In the moment when each reactance is disconnected the voltage increases suddenly and the voltage controller reduces quickly the voltage to its nominal value by absorbing reactive power.

In order to illustrate the PMSG wind turbines' voltage grid support capability in a large power system, an extended model of the test model for the power transmission system described in [29] and shown in Figure 24, is used in the following. The test model illustrated in Figure 43 is used, but this time the new added wind farm is made up exclusively of PMSG wind turbines. The new wind farm consists of 80 equal 2MW DFIG wind turbines. Similar to the case of DFIG wind farm, discussed in Section 7.2, PMSG wind farm is connected to the transmission system at a 135 kV busbar through an offshore line just like in the connection case of the offshore active stall wind farm. The new wind farm is modelled based on the aggregation technique, namely by one equivalent lumped wind turbine with re-scaled power capacity. It is thus assumed that, during the grid fault, the PMSG wind farm operates at its rated capacity. The wind farm is modeled with a one-machine approach based on the aggregation technique.

In Figure 48, the voltage, the active power and the reactive power of the PMSG wind farm in the wind farm terminal (WFT) are illustrated. Two situations are compared: with and without voltage control of the PMSG wind farm, respectively. In order to achieve and illustrate the worst case for voltage stability, it is assumed that the power reduction control of the active stall wind farm is completely disabled during this first simulation.

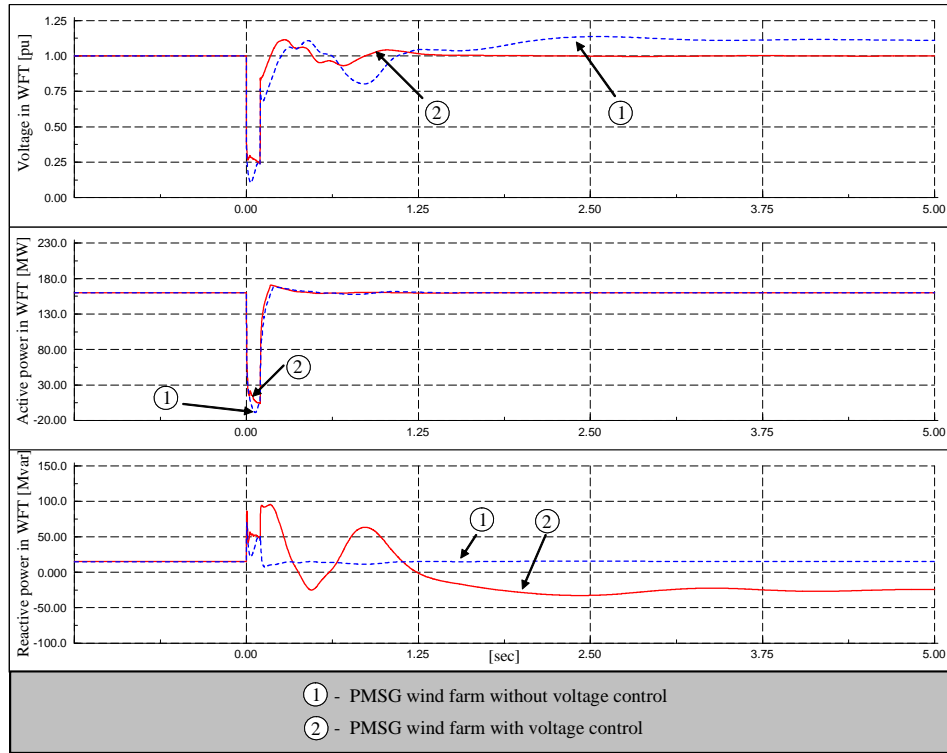


**Figure 48: PMSG wind farm terminal (WFT) with and without voltage control when the power reduction control of the active stall wind farm is disabled.**

Notice that the grid fault causes a severe voltage drop at the wind farm terminal. As expected, the influence of PMSG wind farm's voltage control is visible both during the fault and after the fault is cleared (i.e. the voltage level is improved in both cases). When no voltage control is enabled, the grid voltage oscillates longer and stabilizes to a higher voltage level after the fault is cleared. This can be explained both by the reactive power surplus existent in the system as result of the on-land wind turbines disconnection and by the fact that, as result of the fault clearance (tripping Line 4), the transport of the active power from the wind farms to the grid is done through a higher resistance transmission line. Figure 48 shows that, when the voltage control is enabled, the existing reactive power surplus in the system after the fault is absorbed by the PMSG wind farm. The



PMSG wind farm equipped with voltage control manages thus to re-establish quickly the grid voltage to 1p.u. by controlling the reactive power supply. Notice that, as expected, there is no significant effect of the voltage control on the active power production.

## 8. Conclusions

This report presents the results of several detailed investigations regarding the impact on large power systems of different wind turbine concepts like active stall induction generator (ASIG) wind turbines, doubly-fed induction generator (DFIG) wind turbines and multi-pole permanent magnet synchronous generator (PMSG) wind turbines. The attention is drawn to the most relevant features regarding integration of wind power into large power systems, i.e. fault ride through, power control and voltage support control capabilities of different wind farm concepts.

The presented control strategies for each considered wind turbine concept have been designed to comply with the grid code requirements. The contribution of these wind turbine concepts to grid support has been assessed and discussed by means of simulations with the use of a transmission power system generic model developed and delivered by The Danish Transmission System Operator Energinet.dk. Based on these simulations, the following conclusions can be drawn:

- An active stall wind turbine (ASIG), equipped with an appropriate controller, can provide a relatively fast response to changes in active power demands. Simulations with tuned, stable and fast controllers show that a new active power set point is reached fully within a few seconds. On the reactive power side, if a dynamic phase control, similar to that in the Nysted wind turbines, is used, it is possible to provide immediate response to reactive power demands and therefore the voltage can be controlled very quickly. The immediate response is obtained in the simulations by introducing a hysteresis in the control loop. Alternatively, a low pass filter would be required, which would have slowed down the response.

- The fault ride-through capability of an ASIG wind farm, and thus its stabilization at a short circuit fault, can be achieved by reducing the wind turbine power production for duration of few seconds from the moment of fault occurrence.
- Variable speed wind turbines (DFIG and PMSG) can respond immediately to changes in active as well as reactive power demands. It has been shown, that PMSG wind turbines with full-scale frequency converter have a better grid support capability than DFIG wind turbines with partial-scale frequency converter. Due to the full converter system PMSG wind turbines can provide a higher amount of reactive power to the grid. This yields that the voltage level is supported to a higher level and recovers faster.
- Moreover, both variable speed wind turbine concepts can help the nearby connected stall or active stall wind turbines to ride-through grid faults and can enable them to partly comply with grid code requirements.
- As PMSG wind turbine itself is fully decoupled from the grid by the converter, it is less subjected to the impact of a grid fault. In contrast to this, DFIG wind turbine is direct grid connected generator and it requires therefore an additional protective equipment, as e.g. a crowbar, during grid faults to avoid high transient short circuit currents in the generator rotor. Besides a protection system, a damping controller is also necessary to ensure the DFIG fault ride-through capability. Due to the direct grid connection in DFWG wind turbine concept, the generator, converter and turbine system are directly exposed to the grid fault. As result, strong oscillations in the drive train may appear whenever the system gets excited. This aspect may cause the disconnection of the wind turbine, if no damping controller is activated.
- Full-scale converter multi-pole PMSG wind turbines are able to ride-through grid faults even without additional measures. Nevertheless, the use of a chopper can reduce effectively the grid fault impact on the wind turbine mechanical stress (i.e. smaller oscillations in the shaft torque) and enhances even further the PMSG wind turbine's fault ride-through capability.

## References

- [1] Hansen A. D., Iov F., Blaabjerg F., Hansen L.H. Review of Contemporary Wind Turbine Concepts and their market Penetration. *Wind Engineering*, 2004, Vol. 28, No.3, pp. 247-263.
- [2] Blaabjerg F., Chen Z., Kjaer S.B. Power Electronics as efficient interface in dispersed power generation systems. *IEEE Trans. on Power Electronics*, 2004, Vol.19, No.5, pp.1184-1194.
- [3] Slootweg J. G., Kling W. L., Modelling and analysing impacts of wind power on transient stability of power systems, *Wind Engineering*, 2001, Vol. 25, No.6, pp. 3-20.
- [4] Gjengedal T., Integration of wind power and the impact on power system operation, *IEEE*, 2003, pp. 76-83.
- [5] Iov F., Hansen A. D., Sørensen P., and Cutululis N. A., "Mapping of grid faults and grid codes," Risø report, Risø-R-1617(EN), 2007.
- [6] Hansen A. D., Michalke G., Sørensen P., Lund T., and Iov F., "Co-ordinated voltage control of DFIG wind turbines in uninterrupted operation during grid faults," *Wind Energy*, Vol. 10, No.1, pp.51-68, 2007.
- [7] Kristoffersen J.R., and Christiansen P., "Horns rev offshore windfarm: its main controller and remote control system," *Wind Engineering*, Vol. 27, No. 5, pp. 351-360, 2003.
- [8] Energinet.dk: 'Wind turbines connected to grids with voltages above 100 kV – Technical regulations for the properties and the control of wind turbines', Energinet.dk, Transmission System Operator of Denmark for Natural Gas and Electricity, Technical Regulations TF 3.2.5, 2004, Available: [www.energinet.dk](http://www.energinet.dk), pp. 1-30.
- [9] Sørensen P. E., Cutululis N. A., Lund T., Hansen A. D., Sørensen T., J. Hjerrild, M. H. Donovan, L. Christensen, and H. K. Nielsen, "Power Quality Issues on Wind Power Installations in Denmark," part of: Power Engineering Society General Meeting, 2007. *IEEE* (ISBN: 1-4244-1298-6) (DOI: 10.1109/PES.2007.385924), pp. 2820-2826, 2007.

- [10] Hansen A.D., Sørensen P., Iov F., and Blaabjerg F., “Grid support of a wind farm with active stall wind turbines and AC grid connection,” *Wind Energy*, vol. 6, pp. 341-359, 2006.
- [11] Sørensen, P.; Hansen, A.D.; Rosas, P.A.C., Wind models for prediction of power fluctuations from wind farms. 5. Asia-Pacific conference on wind engineering, Kyoto (JP), 21-24 Oct 2001. *J. Wind Eng.* (2001) , p 9-18
- [12] Sørensen P., Hansen A.D., Janosi L., Bech J., & Bak-Jensen B. “Simulation of interaction between wind farm and power system”. Risø National Laboratory. Risø-R-1281, 2001.
- [13] Øye,& S. (1991). “Dynamic stall - simulated as time lag of separation”. In Vol. *Proceedings of the 4th IEA Symposium on the Aerodynamics of Wind Turbines*, McAnulty, K.F- (Ed.), Rome, Italy.
- [14] Akhmatov V., An aggregated model of a large wind farm with variable-speed wind turbines equipped with doubly-fed induction generators, *Wind Engineering*, Vol 28, No 4, 2004, pp 479-488.
- [15] Poeller M., Achilles S., “Aggregated Wind Park Models for Analyzing Power System Dynamics”, *Fourth International Workshop on Large-Scale Integration of Wind Power and Transmission Networks*, October 20.21, Billund, Denmark, DlgSILENT, 10p.
- [16] Jauch C, Hansen AD, Sørensen P, Blaabjerg F. Simulation model of an active-stall fixed-speed wind turbine controller. *Wind Engineering*, 2004, Vol.28, No.2, pp. 177- 195.
- [17] Akhmatov V., Knudsen H., Nielsen A.H., Pedersen J.K., Poulsen N.K., Modelling and transient stability of large wind farms, *Electrical Power and Energy Systems* 25 (2003), 123-144
- [18] Sørensen P, Iov F, Blaabjerg F, Skaarup J, Test and simulation of dynamic phase compensation from Mita-Teknik A/S, Risø-R-1438 (EN), 2004.
- [19] Hansen, A.D.; Sørensen, P.; Iov, F.; Blaabjerg, F., Control of variable pitch/variable speed wind turbine with doubly-fed induction generator, *J. Wind Eng.* (2004), vol. 28, No. 4, p 411-432
- [20] Heier S. *Grid Integration of Wind Energy Conversion Systems*, 1998, ISBN 0 471

97143.

- [21] Akhmatov V., Analysis of dynamic behavior of electric power systems with large amount of wind power, PhD thesis, 2003, Ørsted DTU.
- [22] Akhmatov V., Variable-speed wind turbines with doubly-fed induction generators. Part II: Power System Stability. Wind Engineering, Vol. 26, No. 3, 2002, pp 171-188.
- [23] Akhmatov V., Variable-speed wind turbines with doubly-fed induction generators. Part IV: Uninterrupted operation features at grid faults with converter control coordination. Wind Engineering, Vol. 27, No. 6, 2003, pp 519-529.
- [24] Eping C., Stenzel J., Poeller M., Mueller H., Impact of Large Scale Wind Power on Power System Stability, Fifth International Workshop on Large-Scale Integration of Wind Power and Transmission Networks, April 7-8, 2005, Glasgow, Scotland, 9p.
- [25] Kayikci M., Anaya-Lara O., Milanovic J.V., Jenkins N., Strategies for DFIG voltage control during transient operation, CIRED, 18th Int. Conference on Electricity Distribution, 2005, Turin, 5p.
- [26] Hansen A.D., Jauch C., Sørensen P., Iov F., Blaabjerg F. Dynamic wind turbine models in power system simulation tool DIgSILENT, Risø-R-1400(EN), 2003.
- [27] P. Kundur, Power System Stability and Control, Ed. McGraw-Hill, 1994.
- [28] Hansen A.D., Michalke G., Multi-pole PMSG wind turbines' grid support capability in uninterrupted operation during grid faults, IET Renewable Power Generation, Vol.3, Issue 3, September 2009, p333-348.
- [29] Akhmatov, V., and Nielsen, A.H.: 'Simulation Model of the Transmission Grid for a Large Offshore Windfarm, Used in Education and Research at the Technical University of Denmark', Wind Engineering, 2006, 30, (3), pp. 255-263.